

University of Dundee

Parametric Study of Nonlinear Wave Loads on Submerged Decks in Shallow Water

Hayatdavoodi, Masoud; Treichel, Kayley ; Ertekin, R. Cengiz

Published in:
Journal of Fluids and Structures

DOI:
[10.1016/j.jfluidstructs.2019.02.016](https://doi.org/10.1016/j.jfluidstructs.2019.02.016)

Publication date:
2019

Licence:
CC BY-NC-ND

Document Version
Peer reviewed version

[Link to publication in Discovery Research Portal](#)

Citation for published version (APA):
Hayatdavoodi, M., Treichel, K., & Ertekin, R. C. (2019). Parametric Study of Nonlinear Wave Loads on Submerged Decks in Shallow Water. *Journal of Fluids and Structures*, 86, 266-289.
<https://doi.org/10.1016/j.jfluidstructs.2019.02.016>

General rights

Copyright and moral rights for the publications made accessible in Discovery Research Portal are retained by the authors and/or other copyright owners and it is a condition of accessing publications that users recognise and abide by the legal requirements associated with these rights.

- Users may download and print one copy of any publication from Discovery Research Portal for the purpose of private study or research.
- You may not further distribute the material or use it for any profit-making activity or commercial gain.
- You may freely distribute the URL identifying the publication in the public portal.

Take down policy

If you believe that this document breaches copyright please contact us providing details, and we will remove access to the work immediately and investigate your claim.

Parametric Study of Nonlinear Wave Loads on Submerged Decks in Shallow Water

Masoud Hayatdavoodi^{a,*}, Kayley Treichel^b, R. Cengiz Ertekin^c

^a*Civil Engineering Department, SSE, University of Dundee, Dundee DD1 4HN, UK*

^b*Ocean Engineering Department, Texas A&M University, Galveston, TX 77553, USA*

^c*College of Shipbuilding Engineering, Harbin Engineering University, Harbin, China*

Abstract

This study is concerned with calculations of nonlinear wave loads on submerged, horizontal decks in shallow water. Solitary and cnoidal wave loads on submerged decks are determined by use of the Level I Green-Naghdi (GN) equations. Results of the GN equations are compared with the linear theory, CFD, and with available laboratory measurements. Variation of the horizontal and vertical wave-induced loads and the overturning moment on submerged decks is studied through an extensive parametric study. In total, 240 cases are considered for cnoidal waves and 84 cases for solitary waves. The variable parameters include the wave height, wave period, deck submergence depth and deck length. Based on the parametric study results, two empirical, design-type equations are suggested for estimating the vertical and horizontal forces on submerged decks. Results of the empirical equations are compared with the available laboratory measurements and CFD calculations and good agreement is observed. Examples are provided to demonstrate the use of the empirical equations for prototype cases. The parametric study and the empirical equations provide engineers with the preliminary determination of wave loads on submerged decks.

Keywords: Wave loads, coastal bridges, submerged deck, solitary wave, cnoidal wave, parametric study, Green-Naghdi equations

*Corresponding author.

Email address: mhayatdavoodi@dundee.ac.uk (Masoud Hayatdavoodi)

1. Introduction

Consider a fully submerged, horizontal, flat deck. Wave motion over the submerged deck induces vertical and horizontal forces and overturning moment on the deck. In almost all practical cases, the wave-induced loads on the submerged deck are inertia dominated and are due to the instantaneous pressure differential around the structure. Of course, the friction between the fluid and the structure also contributes to the loads, however, these viscous forces are negligible, see e.g. the concluding remarks of Hayatdavoodi et al. (2014) and Seiffert et al. (2014).

The wave-induced horizontal force on the submerged deck is due to the pressure differential at the leading and trailing edges of the deck. The presence of the submerged deck modifies the wave field. The regions above and below the deck are separated and may have different pressure distribution at different stages of the wave propagation. This difference of pressure above and below the deck results in the wave-induced vertical force and the overturning moment on the structure.

Wave interaction with submerged horizontal decks is an interesting subject of a number of scientific and engineering problems. Wave loads on submerged decks is a critical topic on the design and analysis of tsunami and storm wave loads on coastal bridge decks. During a storm event, for example, water level rises to a higher elevation due to the storm surge. In the recent hurricane Harvey (2017) in the Gulf of Mexico, for example, storm surge of more than three meters was observed near Port Lavaca (see Needham (2017)). Larger storm surges are observed in other events. During hurricane Katrina (2005), for example, storm surge of about 6.6m was recorded, see Douglass et al. (2006). Coastal bridges may become fully submerged under such extreme storm surges or tsunamis, as it was observed during the 2004 Sumatra earthquake and the subsequent tsunami in the Indian Ocean (see e.g. Iemura et al. (2005); Unjoh (2006), hurricane Katrina (2005) (see e.g. Robertson et al. (2007)), and the 2011 Great East Japan earthquake (see e.g. Kosa (2011); Akiyama et al. (2013)).

Among others, submerged horizontal plates can also be used as wave breakers (Hayatdavoodi et al. (2017b)), or in wave energy converter devices (Carter and Ertekin (2014)), and in hybrid wave breaker-energy converter applications (Graw (1993)). Recently, Hayatdavoodi et al. (2017a) have proposed a fully submerged wave energy device that generates power due to the vertical oscillation of a submerged horizontal plate. Of course, submerged

plates are also used in the offshore industry as a component of fixed or floating structures, see e.g. He et al. (2008) and Tao and Dray (2008).

Wave loads on submerged horizontal decks have been determined through various theoretical and experimental approaches. Previous studies on oscillatory wave forces on submerged decks were mostly motivated by its application in the offshore industry. Linear solutions and ad-hoc relations, similar to that proposed by Morison et al. (1950), were used to approximate the loads. Brater et al. (1958), Herbich and Shank (1970), and Durgin and Shiau (1975), and more recently Rey and Touboul (2011), conducted laboratory experiments on the interaction of sinusoidal waves with submerged horizontal decks in deep or intermediate water.

In shallow water, wave interaction with a submerged plate was studied by Siew and Hurley (1977) and Patarapanich (1984) through an analytical approach based on the linear wave theory. Similar approach was used by, e.g., McIver (1985); Liu and Iskandarani (1991); Kojima et al. (1994), mainly focusing on the wave diffraction by the submerged plate. By use of an eigenfunction expansion method, Guo et al. (2015b) solved the velocity potential to obtain linear wave loads on a fully submerged bridge deck.

Studies on nonlinear wave loads on submerged, horizontal decks in shallow water were undertaken recently. These are mainly motivated by the damage made to the decks of coastal bridges, piers and jetties during the major storm and hurricane events. Nonlinear wave loads on submerged, horizontal decks are studied by use of the Green-Naghdi (GN) equations by Hayatdavoodi and Ertekin (2015b). Computational Fluid Dynamics (CFD) approach is used by Kerenyi et al. (2009); Bricker and Nakayama (2014); Hayatdavoodi and Ertekin (2015a) and Chu et al. (2016), among others, to determine the wave loads on the submerged deck. Laboratory experiments of wave loads on submerged, horizontal decks include, for example, Bradner et al. (2011) and Schumacher et al. (2008) for intermediate and deep water conditions, and Hayatdavoodi et al. (2015b) for shallow waters.

Empirical relations are provided by the American Association of State Highway and Transportation Officials AASHTO (2008) to estimate the wave-induced loads on submerged decks based on a series of numerical simulations. The empirical coefficients, however, were determined through deep- and intermediate-water waves. In a comparative study by Hayatdavoodi et al. (2015a) for wave loads on submerged prototype bridge decks in shallow water (coastal areas), it is shown that AASHTO's relations may underestimate or overestimate the loads by 100%, or sometimes larger magnitudes,

76 when compared with the CFD results.

77 Studies on solitary wave loads on submerged decks are more limited. The
78 laboratory experiment of Kulin (1958) is one of the first of its kind. Recently,
79 and again motivated by the impact of natural extreme events on coastal
80 structures, the solitary wave loads on submerged decks are determined by
81 the GN equations by Hayatdavoodi and Ertekin (2015c), by use of CFD by
82 Hayatdavoodi (2013) and Seiffert et al. (2014), and by the linear long wave
83 approximation by Lo and Liu (2014), and through laboratory experiments
84 by Hayatdavoodi et al. (2014). A recent critical review of wave loads on
85 horizontal decks, whether submerged or above the still-water level (SWL), is
86 provided by Hayatdavoodi and Ertekin (2016), which provides discussion on
87 the analytical, computational, empirical, and experimental approaches used
88 to study this problem.

89 For wave loads on horizontal decks at or above the still-water level, par-
90 ticularly with applications on coastal bridges, see e.g. Xu et al. (2015); Guo
91 et al. (2015a); Azadbakht and Yim (2016); Park et al. (2017).

92 In recent years, there have been significant studies on nonlinear wave
93 loads on submerged horizontal decks. Most of these works, however, are
94 motivated by (i) introducing a new numerical method to determine the wave
95 loads, (ii) applying existing methods to a particular structure under given
96 conditions, or (iii) providing an overall insight to this particular problem
97 through laboratory experiments. Moreover, a majority of the studies have
98 focused on cases where the horizontal decks are located at or above the SWL,
99 mainly because these are the most likely operational conditions. However, in
100 a series of case studies, using various theoretical approaches, Hayatdavoodi
101 et al. (2015a) showed that for a horizontal deck with fixed position, wave
102 loads are always larger when the deck is fully submerged (due to the storm
103 surge). This is mainly because larger waves (with respect to the structures
104 size) may impinge on the deck as the water depth increases due to storm
105 surge. Therefore, at the design and analysis stages, the loads on the fully
106 submerged structure must be considered, if deck inundation is a possibility.

107 Our goal in this work is to study the nonlinear periodic and solitary wave
108 loads on submerged, horizontal decks in shallow water. Variation of the
109 wave loads with the involved variables is of particular interest. Given the
110 recent extreme events around the world, we will consider a range of possible
111 wave and environmental conditions and deck geometries in this study. Our
112 objectives are (i) to perform a parametric study of wave loads on submerged
113 decks and determine the dependency of the loads on the wave conditions and

114 deck geometries, and (ii) to determine empirical relations that can be used
115 to estimate the wave loads on submerged decks.

116 In this study, we use the Level I GN equations to determine the solitary
117 and cnoidal wave loads on submerged decks. The theoretical model is in-
118 troduced in Section 2. This is followed by the dimensional analysis, wave
119 loads presentation, and the parametric study of solitary and cnoidal wave
120 loads in Sections 3 and 4. The two empirical equations for estimating the
121 wave-induced horizontal and vertical forces on submerged decks are intro-
122 duced in Section 6. Results of these empirical equations are compared with
123 the available theoretical and experimental results in Section 7. Along with a
124 discussion of the agreement between the results, this section includes practi-
125 cal examples demonstrating the use of the empirical equations. This paper
126 is closed by some concluding remarks.

127 2. The Green-Naghdi Equations

128 We assume a flat and stationary seafloor at the vicinity and below the
129 submerged deck. A two-dimensional Cartesian coordinate system, with x
130 pointing to the right and z pointing upward, opposite to the gravitational
131 acceleration, is used. The submerged deck with rectangular cross section is
132 rigid and fixed. A schematic of the problem is shown in Fig. 1.

133 The GN equations for propagation of nonlinear water waves were origi-
134 nally developed based on the theory of directed fluid sheets by Green and
135 Naghdi (1974, 1976). In this theory, the fluid is assumed to be incompressible
136 and inviscid, although viscosity of the fluid is not a constraint in the general
137 form of the theory, see Green and Naghdi (1984). No restriction is made on
138 the irrotationality of the flow.

139 The final form of the Level I GN nonlinear shallow-water wave equations,
140 as used in this study, were first given by Ertekin (1984). These equations, in
141 two dimensions and for a flat and stationary seafloor, are given by

$$\eta_{,t} + \{(h + \eta)u\}_{,x} = 0, \quad (1a)$$

$$\dot{u} + g\eta_{,x} = -\frac{1}{3}\{(2\eta_{,x}\ddot{\eta}) + (h + \eta)\ddot{\eta}_{,x}\}, \quad (1b)$$

142 where $\eta(x, t)$ is the surface elevation measured from the still-water level
143 (SWL), $u(x, t)$ is the horizontal particle velocity, h is the water depth and g
144 is the gravitational acceleration. The atmospheric pressure is assumed zero.

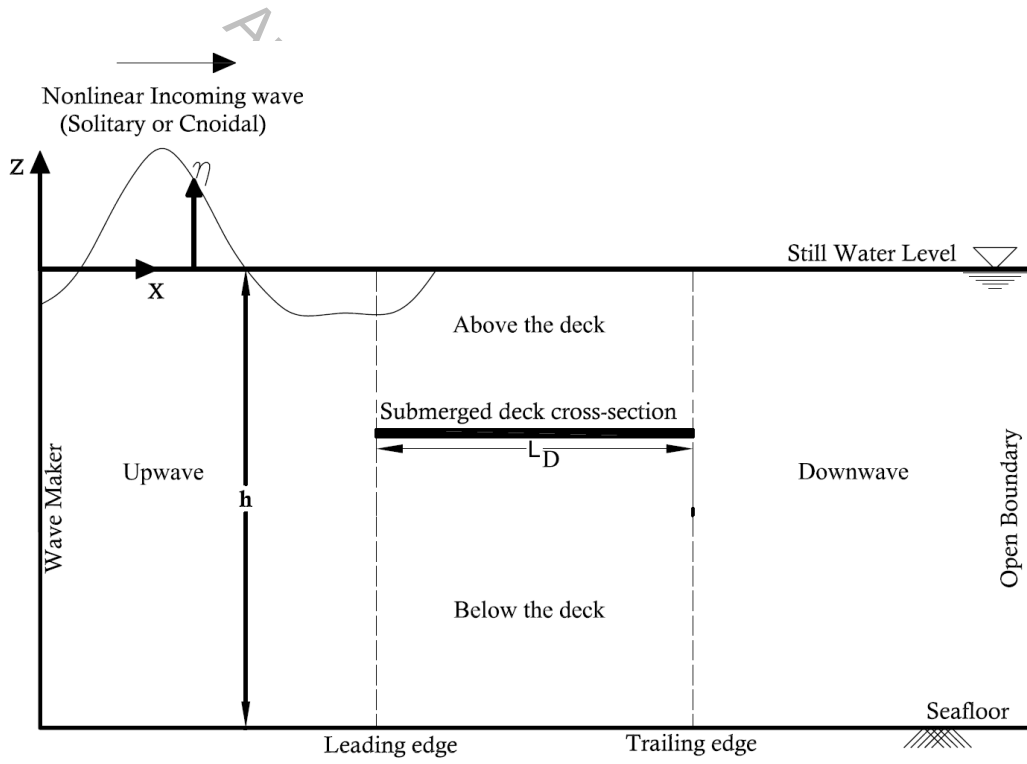


Figure 1: Schematic of the numerical tank of wave interaction with a submerged deck, showing the coordinate system, the submerged deck, and some of the involved parameters.

145 Superposed dots in Eq. (1) denote the material time derivative and double
146 dots are defined as the second material time derivative. All lower case sub-
147 scripts after commas in Eq. (1) designate partial differentiation with respect
148 to the indicated variables. The function η is single-valued, and hence wave
149 breaking is not allowed in this study. Further detail about the GN equations
150 can be found in e.g., Ertekin et al. (1986).

151 The GN equations have been used to study many wave-structure interac-
152 tion problems, see e.g. Neill et al. (2018) and Hayatdavoodi et al. (2018) for
153 solitary and cnoidal wave loads on vertical cylinders, and comparisons with
154 laboratory experiments, Boussinesq equations, and linear solutions.

155 Hayatdavoodi (2013) developed a nonlinear shallow-water model based
156 on the Level I GN equations to calculate the horizontal and vertical wave
157 forces and overturning moment on a fully submerged deck located in water
158 of finite depth. In this approach, the deck is assumed thin and the domain is
159 divided into four regions, namely, upwave and downwave of the submerged
160 deck, above the deck and below the deck. Each region is subject to specific
161 boundary conditions: the nonlinear free surface and the seafloor boundary
162 conditions in the upwave and downwave regions, the nonlinear free surface
163 and the body boundary condition in the region above the deck, and the body
164 and seafloor boundary conditions in the region under the deck. The upwave
165 and downwave boundaries are also subject to the wave making and wave ab-
166 sorbing boundary conditions, respectively. At the discontinuity lines where
167 the boundaries meet, the leading and trailing edge of the deck, jump and
168 matching conditions are applied to obtain a continuous solution throughout
169 the domain. The equations are solved by use of the central-difference ap-
170 proach. Details about the model can be found, for example, in Hayatdavoodi
171 and Ertekin (2015b).

172 Results of this model were compared with the laboratory measurements
173 of solitary and periodic waves and showed a close agreement for a range of
174 parameters, see Hayatdavoodi and Ertekin (2015c) and Hayatdavoodi and
175 Ertekin (2015a). In the GN model, it is assumed that water is always in
176 contact with the submerged deck, i.e., air entrapment is not allowed. That
177 is, we assume that air pockets are relieved as the deck becomes submerged
178 due to the gradual increase of the water level.

179 Unlike the water wave theories based on the perturbation expansion, there
180 are no scaling parameters in the GN model. In absence of any scaling pa-
181 rameter, it is not possible to define the analytical order of error of the equa-
182 tions, in their original form. Hence, applicability and accuracy of the GN

equations to various fluid flow and wave conditions are often determined through comparison with laboratory experiments. See, for example Webster and Wehausen (1995) and Webster and Zhao (2018) for further discussion. Of course, the order of error of the numerical solutions of the GN equations can be determined based on the order of the numerical schemes.

It is, however, possible to approximate the order of error of the GN equations. This can be accomplished by obtaining relations between the GN equations and other nonlinear, shallow-water wave equations. Ertekin (1984), for example, defined a single perturbation parameter (δ , a *small* dimensionless parameter) and used a formal expansion procedure to show that the GN equations can be reduced to other Boussinesq-class equations, (e.g. equations given by Wu and Wu (1982), the original Boussinesq equations Boussinesq (1871), and the equations given by Whitham (1974) and Schember (1982)) when $O(\delta^2)$ and higher order terms are discarded. See Chapter 4 of Ertekin (1984).

3. Dimensional Analysis

Variation of the wave-induced loads on submerged decks with the environmental conditions and deck characteristics is studied in this work. The environmental conditions include wave height (H), wave period (T) and the water depth (h). The deck characteristics include the elevation of the deck from the seafloor (E_D), and the deck length (L_D), in the direction of wave propagation. Instead of E_D , we use the submergence depth defined as the depth from the SWL to the deck, i.e. $S = h - E_D$.

The deck thickness (t_D) is not a variable since in the GN equations the deck is assumed very thin compared with the other dimensions. Previous studies, using laboratory measurements and various theoretical approaches, have shown that the thickness of the deck for typical structures does not play a significant role on the two-dimensional wave-induced loads. For example, shown in Figs. 18 and 19 of Hayatdavoodi et al. (2014), the peaks of dimensionless solitary wave horizontal and vertical forces (in the form used here) remain invariant with the change of the deck thickness, even when the deck thickness is about 60% of the water depth. In a similar study, but for cnoidal waves, Hayatdavoodi and Ertekin (2015a) used the GN model and compared the dimensionless horizontal force on a thin plate with that on a deck whose thickness is more than 70% of water depth (determined through laboratory measurements and calculated by an inviscid CFD solver), and showed that

219 the peak of the force remains invariant; see e.g. Fig. 7 of Hayatdavoodi and
220 Ertekin (2015a).

221 Hence, typical deck thicknesses do not alter the dimensionless wave-
222 induced forces on submerged decks considered here. Note that in this study,
223 the two-dimensional vertical force is given as force per unit width (into the
224 page) of the deck, and the horizontal force is given as the force per unit width
225 and unit thickness of the deck. In other words, pressure at the leading and
226 trailing faces of the deck is almost uniform. Thickness includes both deck
227 and girders, if exist. Care should be given in extending such assumptions to
228 decks located at or near (above or below) the free surface. Those case may
229 result in wave breaking which changes the wave dynamics.

230 We assume $F_x = f_1(h, H, T, S, L_D)$, where F_x is the horizontal force
231 and f_1 is an unknown function. Similarly, $F_z = f_2(h, H, T, S, L_D)$ and
232 $M_y = f_3(h, H, T, E_D, L_D)$ where F_z and M_y are the vertical force and over-
233 turning moment, respectively, and f_2 and f_3 are unknown functions. One of
234 the objectives in this study is to determine approximate solutions to f_1 , f_2
235 and f_3 . The overturning moment, in this study, is calculated with respect
236 to the middle point of the deck. Selection of this point is arbitrary, how-
237 ever, different overturning moment could easily be calculated for different
238 reference points. Here, waves propagate in the positive x direction, and pos-
239 itive and negative overturning moments, respectively, refer to clockwise and
240 counterclockwise moments with respect to the middle of the deck.

241 Loads and parameters are nondimensionalized with respect to the water
242 density (ρ), gravity (g), and water depth (h), which form a dimensionally
243 independent set of variables. The two-dimensional horizontal (F_x) and verti-
244 cal (F_z) forces and the overturning moment (M_y) are given in dimensionless
245 form by

$$\bar{F}_x = \frac{F_x}{\rho g h t_D B_D}, \quad \bar{F}_z = \frac{F_z}{\rho g h^2 B_D}, \quad \bar{M}_y = \frac{M_y}{\rho g h^3 B_D}, \quad (2)$$

246 where B_D is the deck width, into the page. The over bars indicate the
247 dimensionless variables. The dimensionless time (and wave period) is given
248 by

$$\bar{t} = t \sqrt{\frac{g}{h}}. \quad (3)$$

249 The wave height and amplitude, wavelength and submergence depth are
250 nondimensionalized with respect to the constant water depth, i.e., $\bar{H} = H/h$,

251 $\bar{A} = A/h$, $\bar{\lambda} = \lambda/h$ and $\bar{S} = S/h$. Similarly, deck length is given by $\bar{L}_D =$
 252 L_D/h .

253 All results are given in dimensionless form unless otherwise stated. For
 254 simplicity, bars are removed hereon from all dimensionless variables and
 255 loads.

256 Aside from Buckingham's Pi Theorem used above, other approaches may
 257 be used to determine a dimensionless relation between desired functions (usu-
 258 ally pressure or velocity) with the corresponding variables, see for example
 259 Zitti et al. (2016).

260 4. Wave loads on submerged decks

261 The results of the GN equations for wave loads on submerged decks are
 262 presented in this section. All results in this study are given in two-dimensions,
 263 assuming incident waves approach the deck perpendicularly. This gives a
 264 conservative result for the wave loads. However, if the waves approach the
 265 deck at an angle of θ different from zero, one can use the present results and
 266 vector calculus to determine the force component F_y easily.

267 Time series of oscillatory wave loads on a submerged, horizontal deck are
 268 presented in Fig. 2. The results of the GN model are compared with two
 269 linear solvers of the problem, namely the long-wave approximation (LWA)
 270 of Siew and Hurley (1977), and HYDRAN, a computational solver based
 271 on the Green function method, see HYDRAN (2012), Ertekin et al. (1993)
 272 and Riggs et al. (2008). In this comparison, the wave height $H = 0.3$,
 273 wave period $T = 11.5$, submergence depth $S = 0.5$ and the deck length is
 274 $L_D = 3$. Periodic linear waves are generated in the linear solvers. Overall,
 275 good agreement is observed between the models. The loads, particularly
 276 the vertical force, are nonlinear. The LWA significantly overestimates the
 277 vertical force amplitude, as seen in Fig. 2.

278 The uplift forces and the downward force correspond to the maximum
 279 and minimum values of the vertical force on the submerged deck, respec-
 280 tively. Similarly, the positive and negative horizontal forces correspond to
 281 the maximum and minimum horizontal forces, respectively. These are shown
 282 in Fig. 2. In the following sections, these maximum and minimum forces are
 283 presented.

284 Further comparison of the GN results with HYDRAN, as well as other
 285 theoretical and experimental data, can be found in Hayatdavoodi and Ertekin

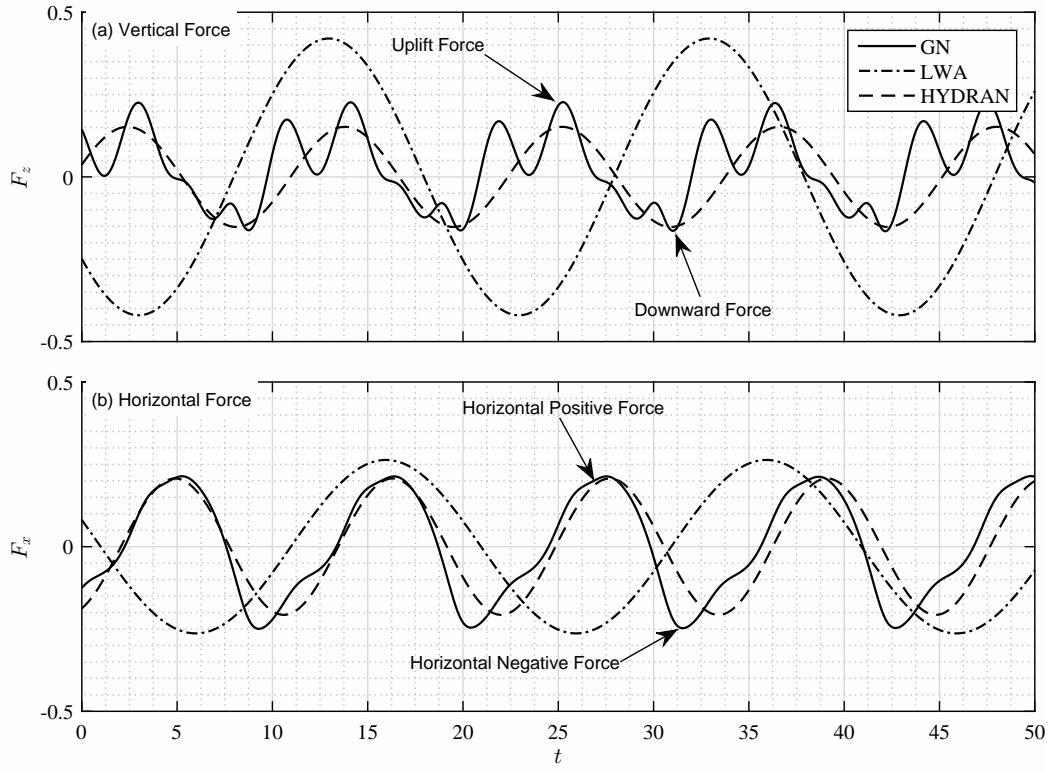


Figure 2: Time series of (a) horizontal and (b) vertical forces on a submerged deck, calculated by the GN equations, and the linear solutions of HYDRAN and LWA. Also shown in this figure are the maximum and minimum values of the horizontal force (horizontal positive and horizontal negative) and the vertical force (uplift and downward), as referred to in the text.

Table 1: Range of the parameters used in the parametric study.

	Wave Height	Wave Period	Submergence Depth	Deck Length	Total Cases
Solitary Wave	$0.1 < A < 0.5$	NA	$0.2 < S < 0.8$	$1 < L_D < 7$	84
Cnoidal Wave	$0.05 < H < 0.45$	$5 < T < 30$	$0.2 < S < 0.8$	$1 < L_D < 7$	240

(2015c). In Section 7, comparison of the GN results with laboratory experiments and some computational solvers are shown.

5. Parametric Study of Wave Loads

Variation of the wave-induced loads on a submerged horizontal deck with wave conditions and deck geometry is presented in this section. Based on the previous extreme environmental conditions, a range of parameters is considered. For periodic waves, in the dimensionless form, these include $0.05 < H < 0.45$, $5 < T < 30$, $0.2 < S < 0.8$ and $1 < L_D < 7$. For solitary waves, $0.1 < A < 0.5$ is considered, where A is the solitary wave amplitude. In some cases, the upper or lower limit of the variables cannot be used, and these are discussed in the following subsections. In total, 84 cases are considered for the solitary wave and 240 cases for cnoidal waves. The range of the variables are summarized in Table 1. Results of the solitary wave loads are presented first, followed by cnoidal wave cases. All results in this section are obtained by the GN equations.

5.1. Solitary Wave

5.1.1. Wave Loads vs. Amplitude

In this section, the variation of solitary wave loads versus wave amplitude (A) on decks of three different lengths ($L_D = 1, 5, 10$) submerged at two different depths ($S = 0.5, 0.8$) is studied. The amplitude varies from $A = 0.1$ to $A = 0.5$ with 0.1 intervals. The results are shown in Figs. 3-5.

For all deck lengths, the vertical force increases linearly with the wave amplitude. The length of the deck affects the force more than the submergence

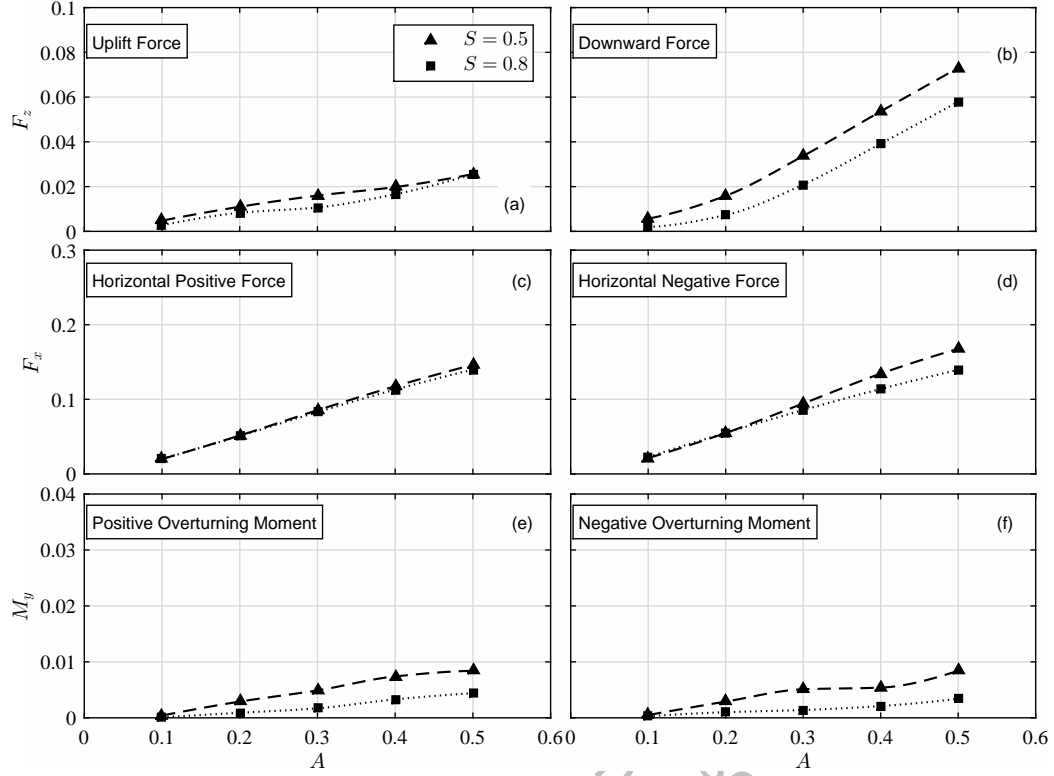


Figure 3: (a) Vertical uplift, (b) vertical downward, (c) horizontal positive and (d) horizontal negative forces, and (e) positive and (f) negative overturning moment due to solitary wave impact on a submerged deck ($L_D = 1$).

depth (see Figs. 4(a) and 5(a)). Similar to the vertical forces, the horizontal forces increase linearly with the wave amplitude. The submergence depth affects the negative horizontal force more as the deck length increases (see Fig. 5(d)). The overturning moment increases linearly for all deck lengths. The submergence depth influences the overturning moment more at smaller deck lengths (see Figs. 3(e)-5(e)).

5.1.2. Wave Loads vs. Deck Length

The variation of solitary wave loads versus deck length (L_D) for a single wave amplitude ($A = 0.2$) and two submergence depths ($S = 0.5, 0.8$) is studied in this section. The deck length varies from $L_D = 1$ to $L_D = 20$ with an interval of 5. The results are shown in Fig. 6.

The vertical forces increase as the deck length increases. The uplift force

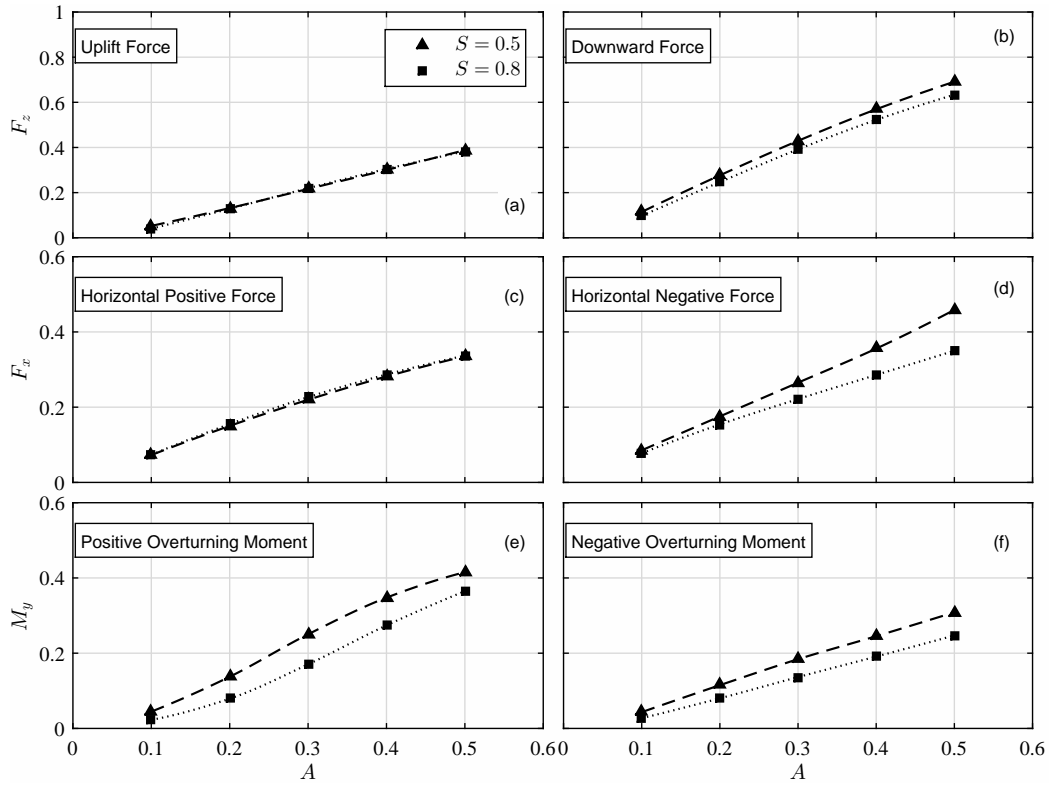


Figure 4: (a) Vertical uplift, (b) vertical downward, (c) horizontal positive and (d) horizontal negative forces, and (e) positive and (f) negative overturning moment due to solitary wave impact on a submerged deck ($L_D = 5$).

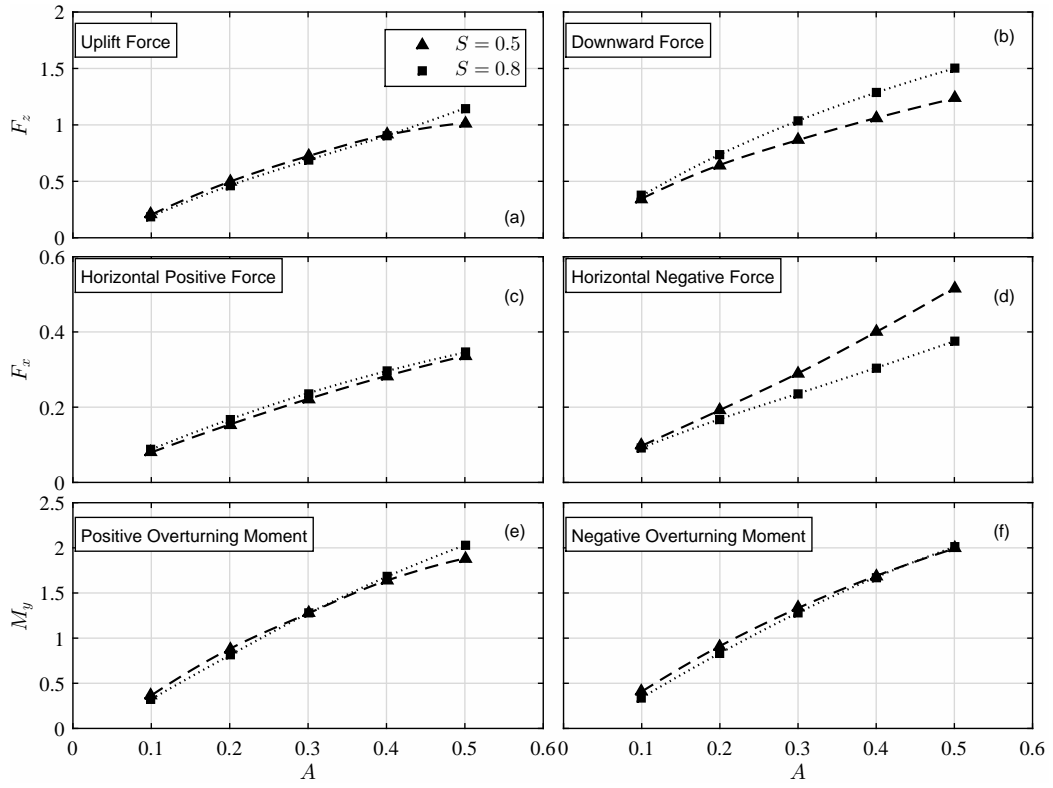


Figure 5: (a) Vertical uplift, (b) vertical downward, (c) horizontal positive and (d) horizontal negative forces, and (e) positive and (f) negative overturning moment due to solitary wave impact on a submerged deck ($L_D = 10$).

321 increases gradually while the downward force approaches a constant value,
 322 the magnitude of which depends on the submergence depth (see Fig. 6(a)
 323 and (b)). This is mainly due to the increasing ratio of the deck length to
 324 the effective length of the solitary wave; the main soliton propagates entirely
 325 over the submerged deck resulting in the maximum downward force. In
 326 these cases, the majority of the downward force is due to the weight of the
 327 wave, located entirely above the deck. The horizontal positive force increases
 328 slightly as the deck length increases but then approaches a constant value
 329 after $L_D \approx 10$. This is the same for the two submergence depths (see Fig.
 330 6(c)). The peak of the horizontal force occurs when the wave crest is at
 331 the leading edge of the deck. The trough of the horizontal force occurs
 332 when the crest of the main soliton is at the trailing edge of the deck. Since
 333 the submergence depth of the deck has a significant effect on soliton fission
 334 (disintegration) above the deck, the value of the horizontal negative forces
 335 are different for the two submergence depths; see Fig. 6(d). The overturning
 336 moment increases nonlinearly as the deck length increases. The positive
 337 overturning moment and negative overturning moment have similar values
 338 at the same deck lengths (see Figs. 6(e) and (f)).

339 5.1.3. Wave Loads vs. Submergence Depth

340 In this section, the variation of solitary wave loads versus submergence
 341 depth S for a single wave amplitude ($A = 0.2$) and three deck lengths ($L_D =$
 342 $1, 5, 15$) is studied. The submergence depth varies from $S = 0.2$ to $S = .9$
 343 with an interval of 0.1 . The results are shown in Fig. 7.

344 The vertical force approaches a constant value as the submergence depth
 345 increases mainly because of the smaller variation of pressure at deeper sub-
 346 mergence depths. In the case of a long deck, the downward force increases
 347 with deeper submergence depth (see Fig. 7(b)). This is mainly due to the
 348 significant effect of a long deck on the solitary wave diffraction. As the sub-
 349 mergence depth increases, the wave undergoes less deformation and the main
 350 soliton keeps its form above the deck resulting in a larger downward force.
 351 The horizontal force stays constant for shorter deck lengths. For longer deck
 352 lengths, as the submergence depth increases, the horizontal positive force and
 353 horizontal negative force increase and decrease, respectively (see Fig. 7(c)
 354 and (d)). The variations, however, are very small. This behavior is mainly
 355 due to lesser effect of the deck on the wave at larger depths. In all cases,
 356 the positive overturning moment reduces with the submergence depth, due
 357 to the reduction of the spatial pressure differential around the deck. The

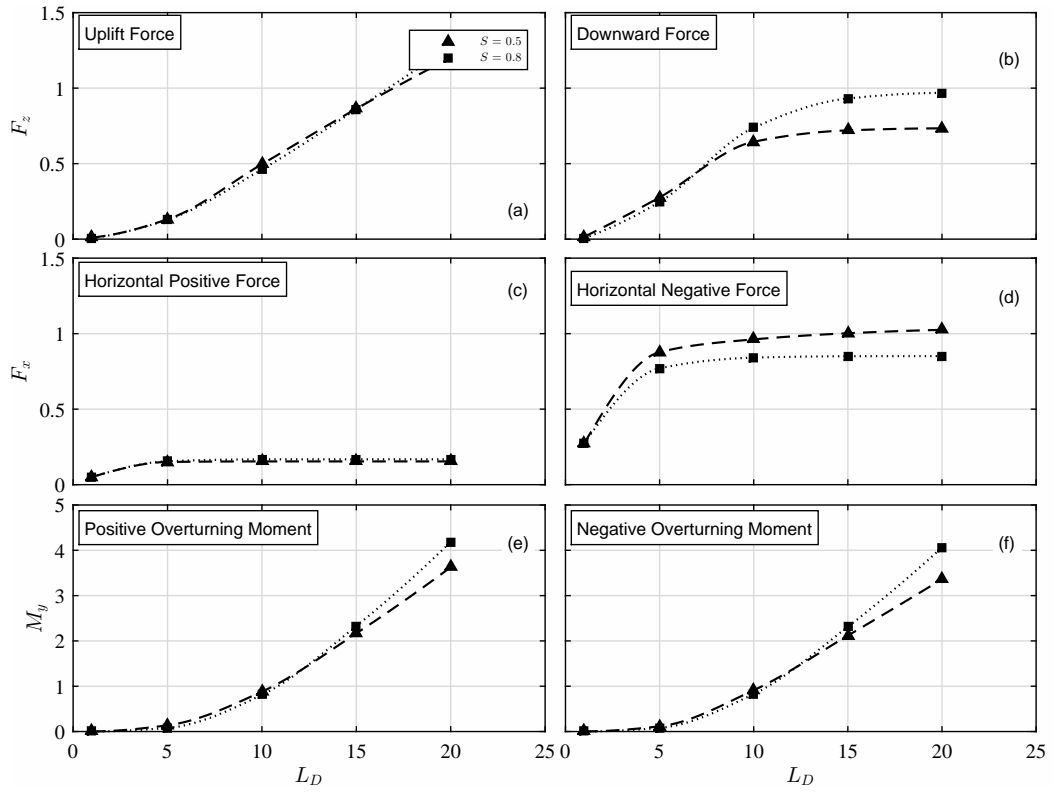


Figure 6: (a) Vertical uplift, (b) vertical downward, (c) horizontal positive and (d) horizontal negative forces, and (e) positive and (f) negative overturning moment due to solitary wave impact on a submerged deck ($A = 0.2$).

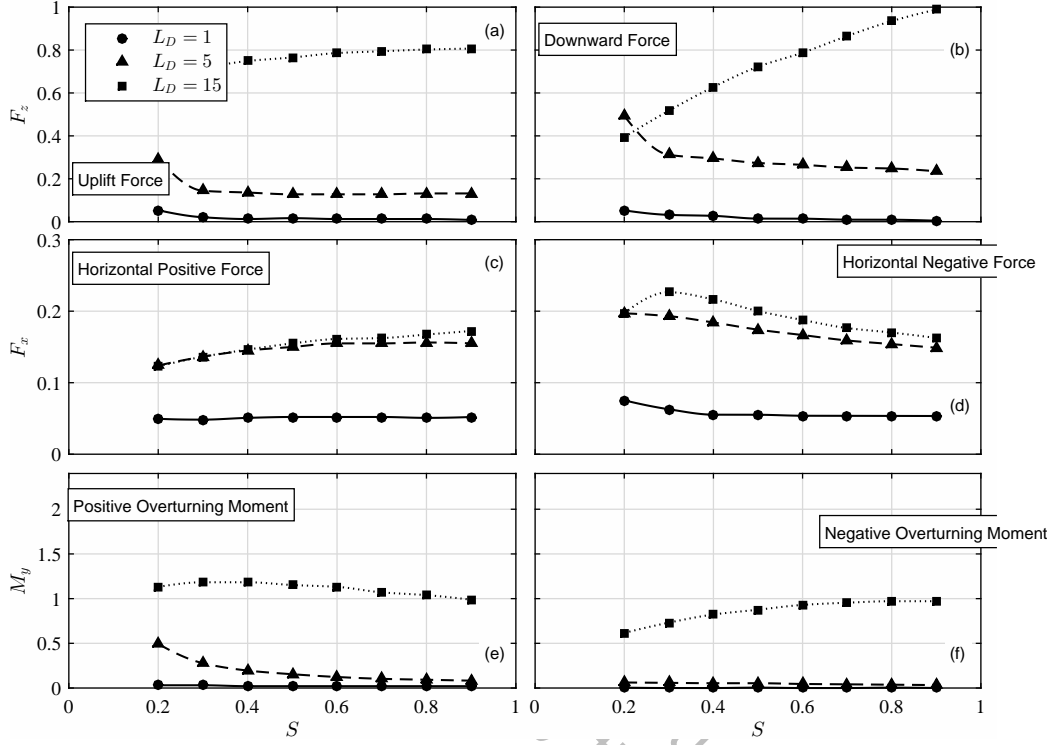


Figure 7: (a) Vertical uplift, (b) vertical downward, (c) horizontal positive and (d) horizontal negative forces, and (e) positive and (f) negative overturning moment due to solitary wave impact on a submerged deck ($A = 0.2$).

change in the positive overturning moment is less significant when the deck is submerged beyond $S \approx 0.5$ (see Fig. 7(f)). The overturning moment for short deck lengths is very small compared with the overturning moment for longer deck lengths, and this is not remarkable.

5.2. Cnoidal Waves

5.2.1. Wave Loads vs. Wave Height

In this section, variation of the cnoidal wave loads versus wave height (H) on a deck of constant length ($L_D = 4$), submerged at three different depths ($S = 0.3, 0.5, 0.7$) and for three wave periods ($T = 7.5, 15, 22.5$) is studied. The results are given in Figs. 8-10. The largest wave height ($H = 0.45$) is eliminated for the shallowest submergence depth ($S = 0.3$, see Fig. 8) due to the wave breaking over the model.

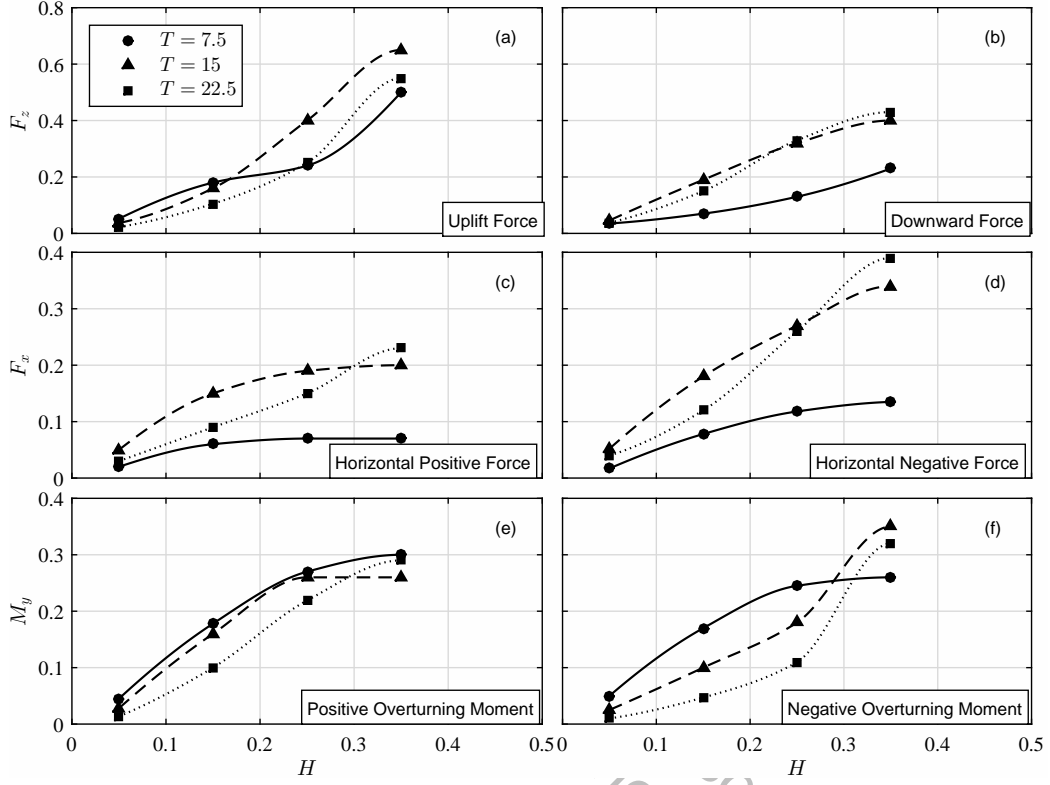


Figure 8: (a) Vertical uplift, (b) vertical downward, (c) horizontal positive and (d) horizontal negative forces, and (e) positive and (f) negative overturning moment due to cnoidal wave impact on a submerged deck ($L_D = 4$; $S = 0.3$).

370 The vertical force increases nonlinearly with the wave height. At smaller
 371 submergence depths, the effect of the wave height on the vertical force is more
 372 significant; see Fig. 8(a). The horizontal force generally increases with larger
 373 wave heights. For smaller periods, the horizontal force increases quickly to a
 374 maximum value, that is considerably less than the values for the larger wave
 375 periods (see Fig. 9(c), for instance). In all cases, and for $T = 7.5$ for example,
 376 the wave height appears to have little to no effect on the horizontal positive
 377 force. This is mainly due to the wave length to deck length ratio of this case,
 378 which results in the simultaneous appearance of the wave crest at the leading
 379 and the trailing edges. This will be discussed further in Subsection 5.2.3. The
 380 overturning moment increases monotonically with the wave height. This is
 381 seen clearly for larger submergence depths (Fig. 10 (f), for example).

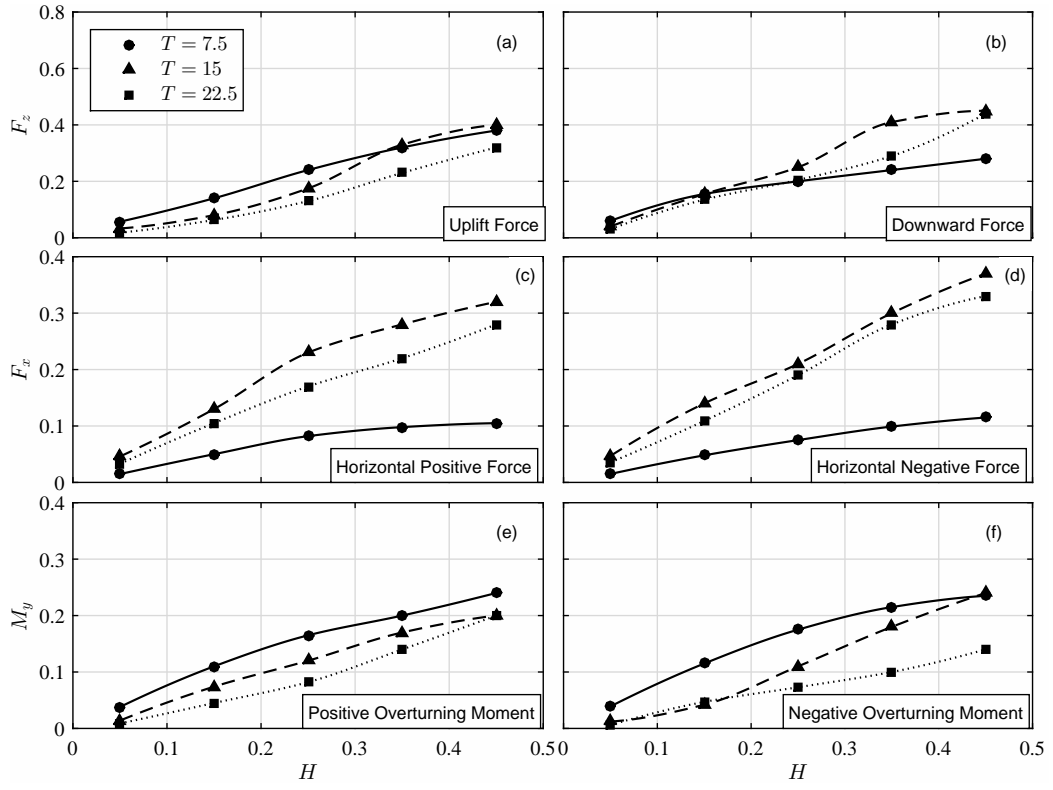


Figure 9: (a) Vertical uplift, (b) vertical downward, (c) horizontal positive and (d) horizontal negative forces, and (e) positive and (f) negative overturning moment due to cnoidal wave impact on a submerged deck ($L_D = 4$; $S = 0.5$).

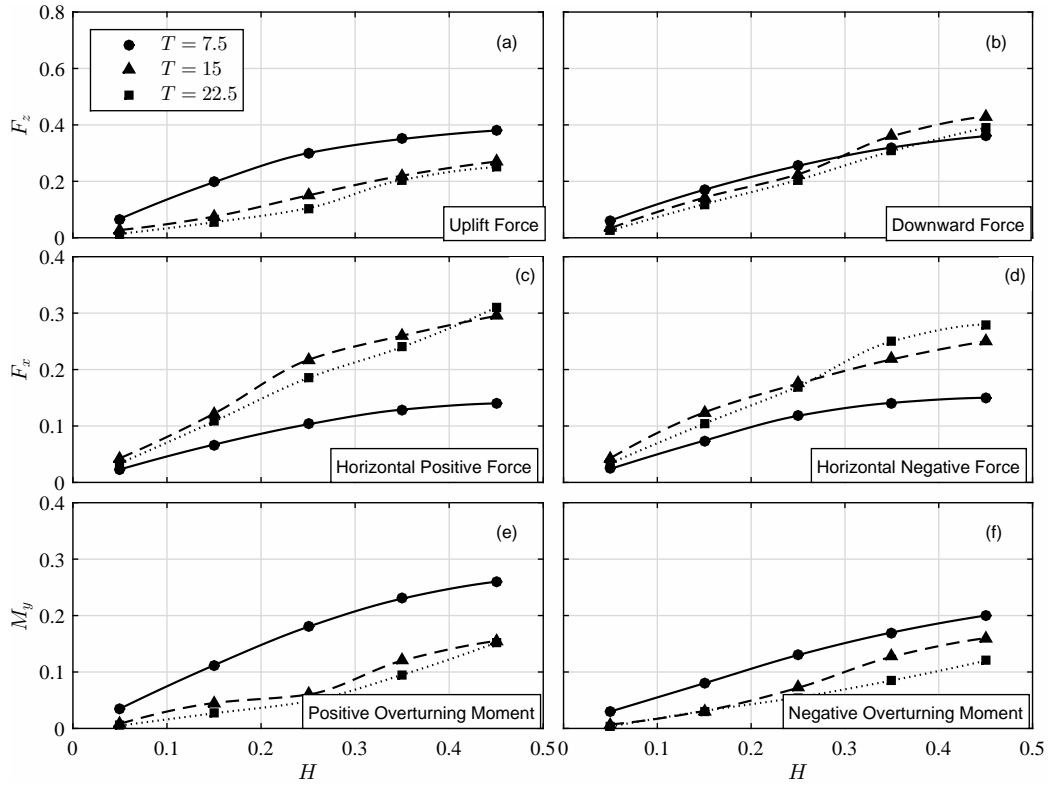


Figure 10: (a) Vertical uplift, (b) vertical downward, (c) horizontal positive and (d) horizontal negative forces, and (e) positive and (f) negative overturning moment due to cnoidal wave impact on a submerged deck ($L_D = 4$; $S = 0.7$).

5.2.2. Wave Loads vs. Submergence Depth

Variation of the cnoidal wave loads against submergence depth (S) of a combination of one wave height ($H = 0.25$), three wave periods ($T = 7.5, 15, 22.5$), and three deck lengths ($L_D = 3, 4, 5$) is given in this section. The submergence depth varies from $S = 0.2$ to $S = 0.8$ with a 0.1 interval. The results are shown in Figs. 11-13.

The vertical forces decrease nonlinearly as the submergence depth increases. For smaller periods, this relationship is oscillatory (see Fig. 13(a)). The horizontal forces appear to approach a constant value after a certain submergence depth. For smaller periods and longer deck lengths, the value of the horizontal force is much smaller than for larger periods at the same deck length (see Fig. 13(c), for example). Again, this suggests that the ratio of wave length to deck length plays a more significant role on the horizontal forces than the wave period (or equivalently wave length) above. The overturning moment generally decreases for larger submergence depths. This relationship is seen better for larger deck lengths (see Fig. 13(e)).

5.2.3. Wave Loads vs. Wave Period

In this section, the variation of the wave loads with wave period for a constant wave height ($H = 0.25$), and a combination of three deck lengths ($L_D = 3, 4, 5$) and three submergence depths ($S = 0.3, 0.5, 0.7$) is presented. The wave period varies between $T = 6$ and $T = 28$ with an interval of 3. The results are shown in Figs. 14-16.

The vertical forces increase steeply from $T \approx 6$ to $T \approx 8$ for larger deck lengths (see Figs. 14(a), 15(a) and 16(a)). Beyond this point, the vertical forces remain nearly constant with the increase in wave period. For the deck lengths considered here, and at $T \approx 6$, there are segments of multiple waves interacting with the deck at the same time. The increase of the period to $T \approx 8$, results in a single wave interaction with the deck at a given time. As the wave period increases beyond this point, the loads mostly remain invariant. The values of the forces for large periods are very close to the solitary wave loads on the bridge deck of the same length and submerged at the same depth. This can be observed by comparing the results given in Figs. 4 and 16 and for $S = 0.5$. The variation of the horizontal forces with wave period show similar overall behavior to that of the vertical force (see Fig. 16(a) and (b)). The overturning moment shows similar behavior as the vertical forces; an oscillatory behavior as the wave period increases i.e., an initial steep increase, followed by nearly constant values for larger periods.

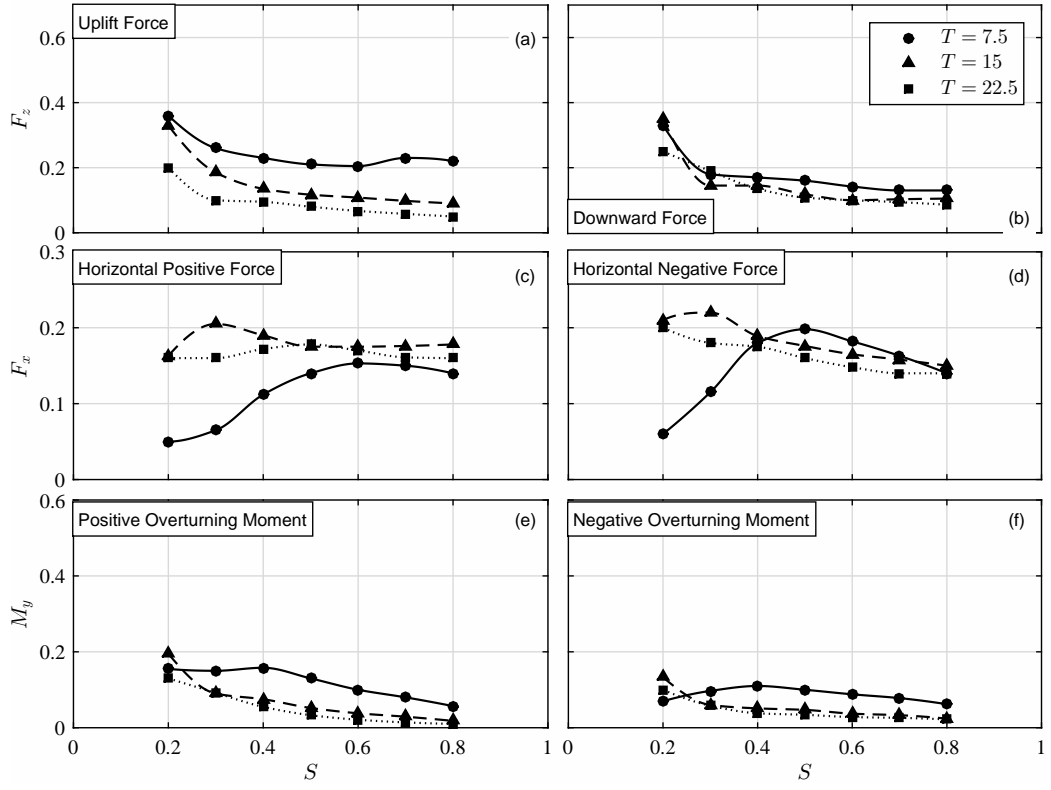


Figure 11: (a) Vertical uplift, (b) vertical downward, (c) horizontal positive and (d) horizontal negative forces, and (e) positive and (f) negative overturning moment due to cnoidal wave impact on a submerged deck ($H = 0.25$; $L_D = 3$).

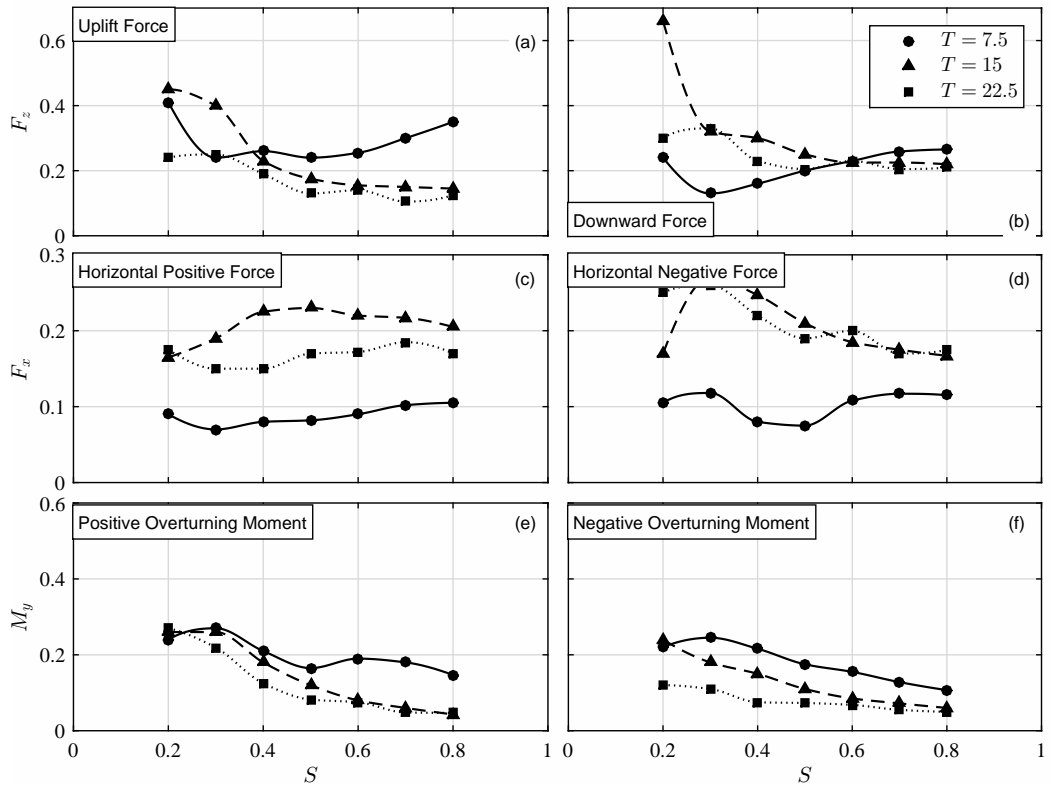


Figure 12: (a) Vertical uplift, (b) vertical downward, (c) horizontal positive and (d) horizontal negative forces, and (e) positive and (f) negative overturning moment due to cnoidal wave impact on a submerged deck ($H = 0.25$; $L_D = 4$).

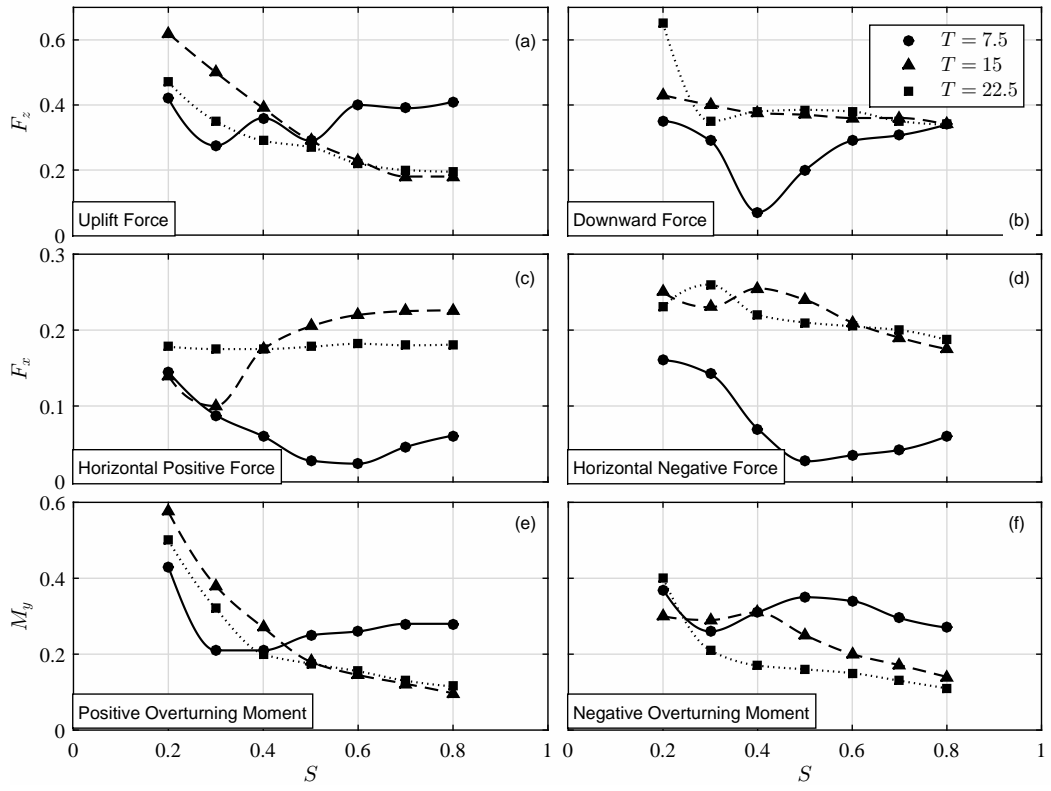


Figure 13: (a) Vertical uplift, (b) vertical downward, (c) horizontal positive and (d) horizontal negative forces, and (e) positive and (f) negative overturning moment due to cnoidal wave impact on a submerged deck ($H = 0.25$; $L_D = 5$).

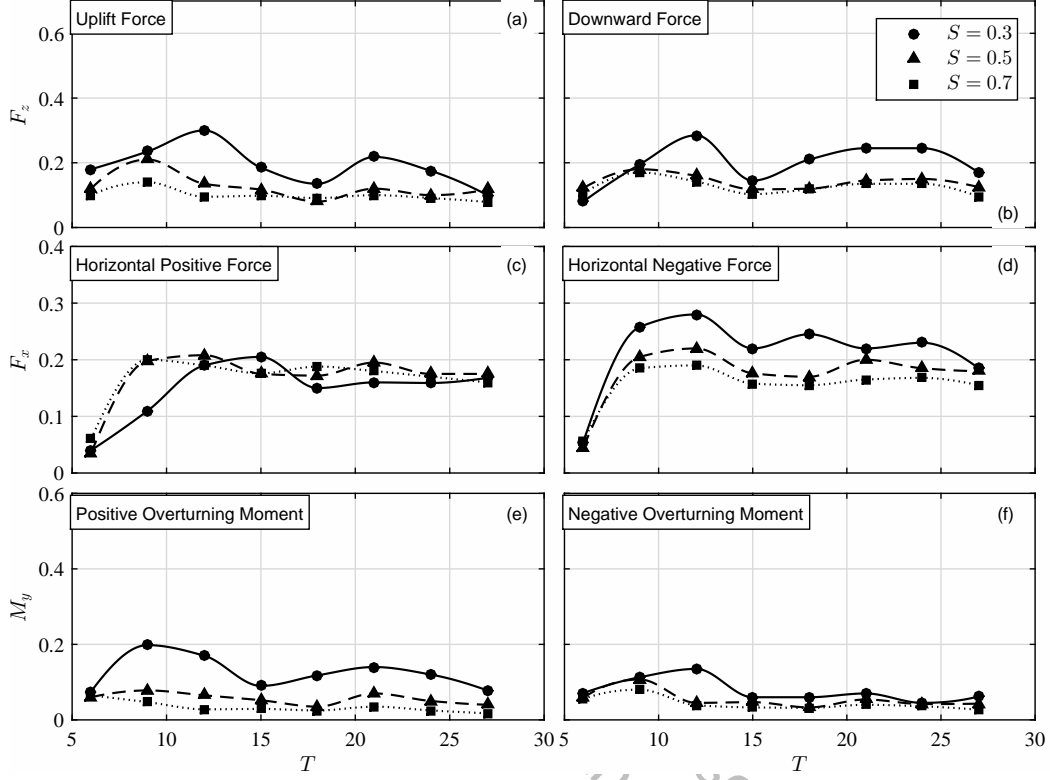


Figure 14: (a) Vertical uplift, (b) vertical downward, (c) horizontal positive and (d) horizontal negative forces, and (e) positive and (f) negative overturning moment due to cnoidal wave impact on a submerged deck ($H = 0.25$; $L_D = 3$).

419 The value increases for larger decks (see Figs. 14(e)-16(e)).

420 5.2.4. Wave Loads vs. Deck Length

421 Figures 17-19 show the variation of the wave loads versus deck length for
 422 a constant wave height ($H = 0.25$) and a combination of three wave periods
 423 ($T = 7.5, 15, 22.5$) and three submergence depths ($S = 0.3, 0.5, 0.7$). The
 424 deck length varies between $L_D = 1$ and $L_D = 7$ with an interval of 1.

425 The vertical forces increase nonlinearly as the deck length increases. This
 426 relationship is shown best for larger submergence depths and wave periods
 427 (see Figs. 18(a) and 19(a)). The horizontal forces oscillate as the deck length
 428 increases. For larger wave periods, the submergence depth does not alter the
 429 horizontal force as much (see Fig. 18(c)). The overturning moment increases
 430 nonlinearly with the deck length. Smaller submergence depths have a higher

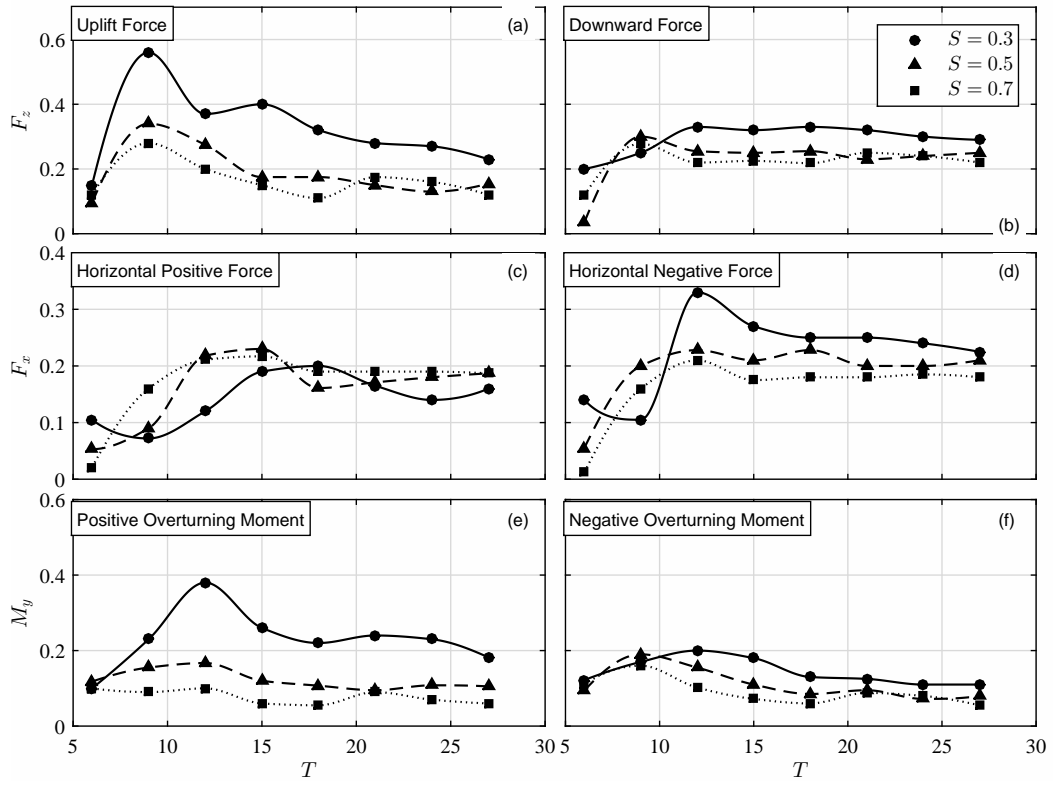


Figure 15: (a) Vertical uplift, (b) vertical downward, (c) horizontal positive and (d) horizontal negative forces, and (e) positive and (f) negative overturning moment due to cnoidal wave impact on a submerged deck ($H = 0.25$; $L_D = 4$).

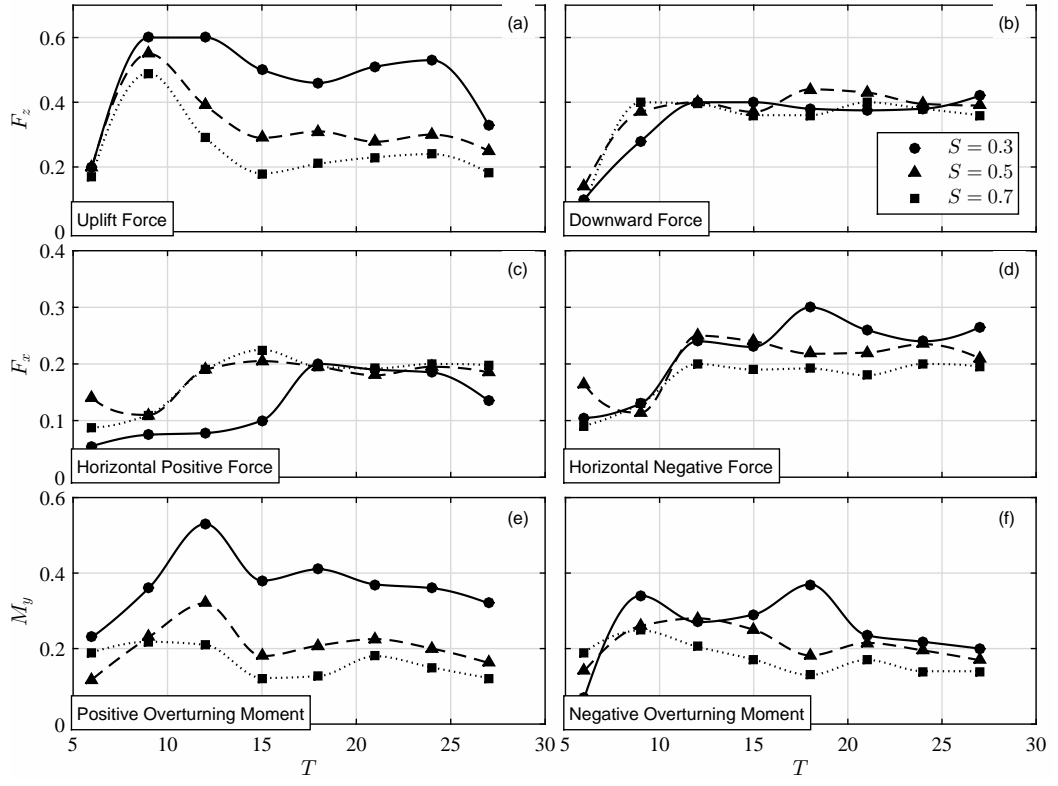


Figure 16: (a) Vertical uplift, (b) vertical downward, (c) horizontal positive and (d) horizontal negative forces, and (e) positive and (f) negative overturning moment due to cnoidal wave impact on a submerged deck ($H = 0.25$; $L_D = 5$).

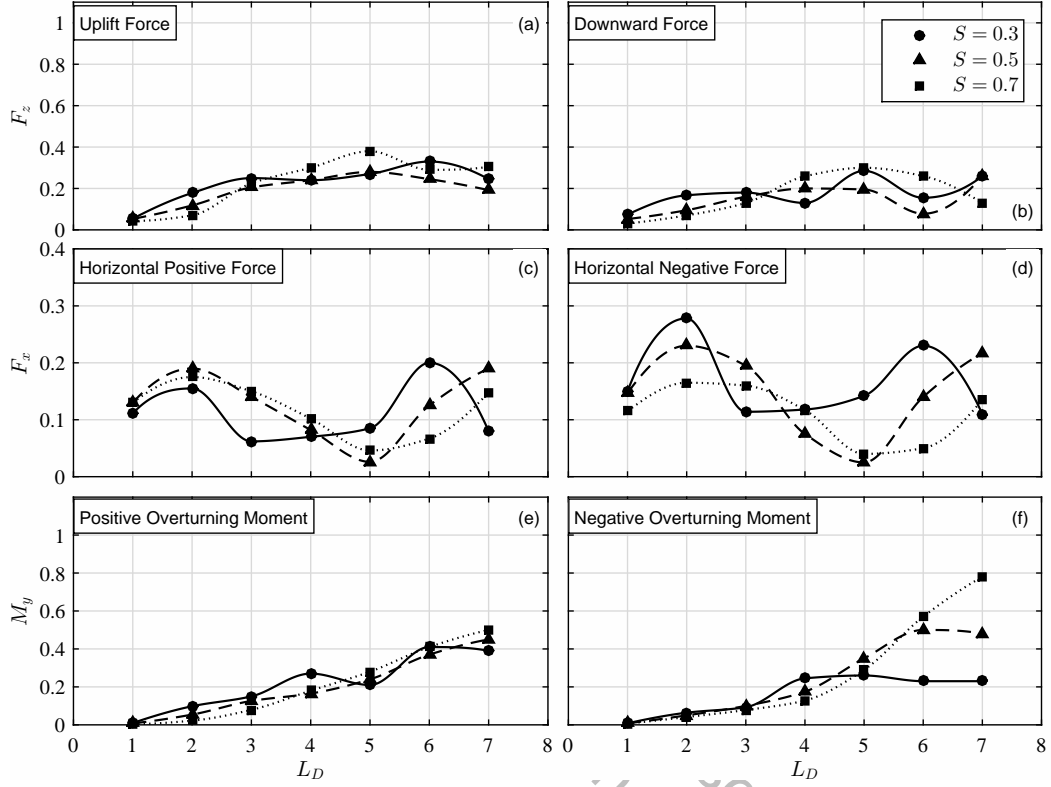


Figure 17: (a) Vertical uplift, (b) vertical downward, (c) horizontal positive and (d) horizontal negative forces, and (e) positive and (f) negative overturning moment due to cnoidal wave impact on a submerged deck ($H = 0.25$; $T = 7.5$).

overturning moment (see Fig. 19(e)).

6. Empirical Equations

Development of design-type empirical equations that could be used to estimate the wave loads on submerged decks is discussed in this section. Only the periodic waves are considered. The vertical uplift and horizontal positive forces are the main load components in practical applications. Hence, the empirical relations are developed for these two forces only.

The form of the empirical equations for the vertical uplift and the horizontal positive forces are determined by analyzing the variation of the forces with wave and deck parameters discussed in Section 5. That is, following the results of the parametric study, it is estimated whether F_z and F_x vary with

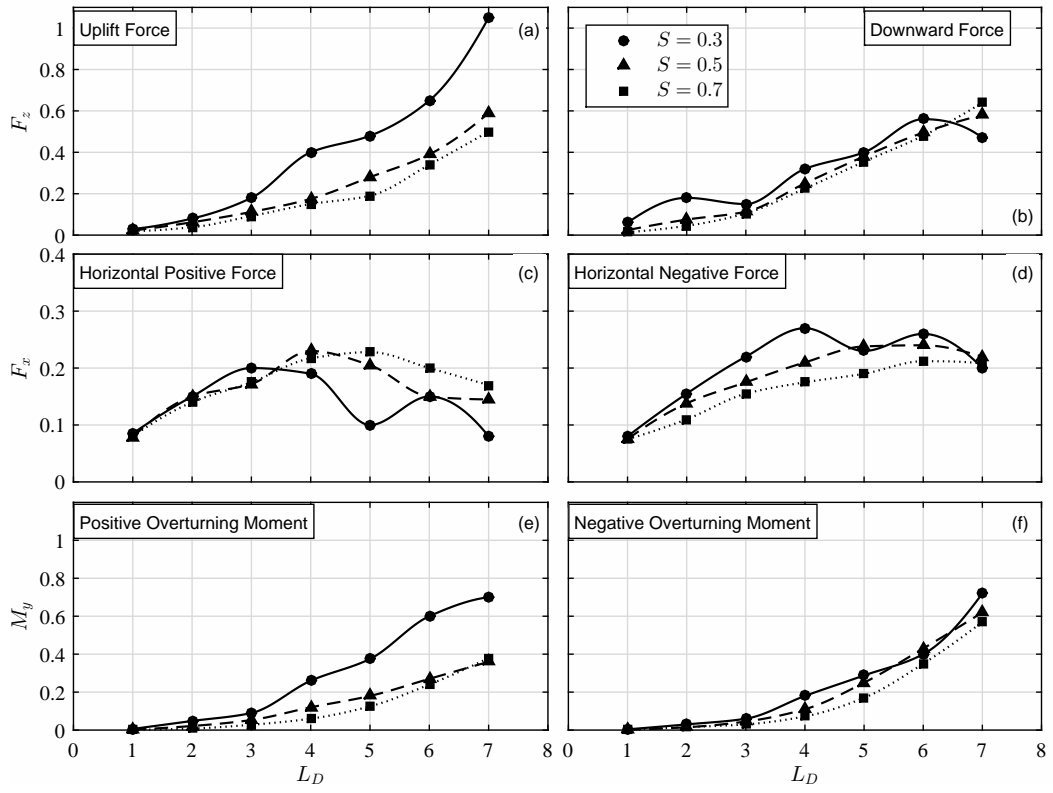


Figure 18: (a) Vertical uplift, (b) vertical downward, (c) horizontal positive and (d) horizontal negative forces, and (e) positive and (f) negative overturning moment due to cnoidal wave impact on a submerged deck ($H = 0.25; T = 15$).

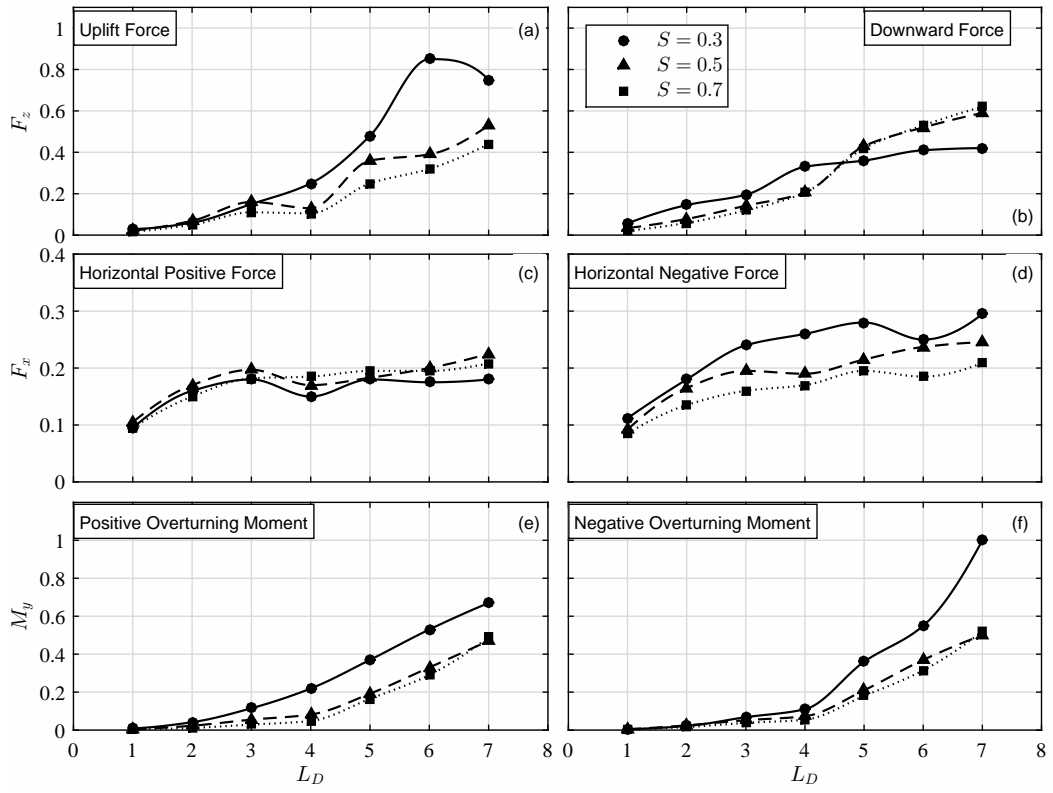


Figure 19: (a) Vertical uplift, (b) vertical downward, (c) horizontal positive and (d) horizontal negative forces, and (e) positive and (f) negative overturning moment due to cnoidal wave impact on a submerged deck ($H = 0.25; T = 22.5$).

442 H , T , S and L_D linearly, exponentially, or logarithmical (or in inverse form
 443 of these functions), subject to unknown, real, empirical coefficients. The val-
 444 ues of the empirical coefficients are determined through regression analysis,
 445 and by use of a *complete search algorithm*. By defining wide, possible ranges
 446 for each of the empirical coefficients, and by use of nested-loops, all possible
 447 combinations of the coefficients are assessed. In determining the values, all
 448 coefficients are considered simultaneously through the search process. In the
 449 nested-loops, intervals of 0.01 are used for each coefficient.

450 The objective of the search algorithm is to determine a combination of the
 451 empirical coefficients that corresponds to smallest *mean absolute error*, when
 452 compared with the results of the GN equations for all cases of the parametric
 453 study. That is, the optimum combination of the coefficients corresponds to
 454 the minimum ϵ defined as

$$\epsilon = \frac{\sum_{i=1}^N |F_{GN} - F_{EE}|}{N}, \quad (4)$$

455 where N is the total number of data points (240 in this study), F_{GN} is the
 456 magnitude of the force (vertical uplift or horizontal positive) calculated by
 457 the GN equations, and F_{EE} is the magnitude of the force estimated by the
 458 empirical equation.

459 The empirical equation for the uplift force is determined as

$$F_z = \frac{0.14(1.68 - S)HL_D^{1.17}}{e^{(0.09L_D)(1.71S - 0.20L_D)}}(1 - e^{-0.64T}). \quad (5)$$

460 The empirical equation for the horizontal positive force is given as

$$F_x = 3.60H^2S^{0.11}(1 - e^{-0.09T})(1 - e^{-L_D}). \quad (6)$$

461 Note that all variables and the forces in Eqs. (5) and (6) are dimensionless
 462 as discussed in Section 3. Also, note that Eqs. (5) and (6) are only applicable
 463 to $S > 0.2$ conditions.

464 The agreement between Eq. (5) and all the GN results for the vertical
 465 uplift force (F_z) is shown in Fig. 20. In this figure, the diagonal dashed line
 466 shows the perfect agreement between the empirical equation and results of
 467 the GN equations. Compared with the GN results, Eq. (5) for the uplift
 468 force has a mean absolute percentage error of 6.15%. Figure 21 shows this
 469 comparison for the horizontal positive force (F_x). The empirical equation for
 470 the horizontal positive force, Eq. (6), when compared with the GN results,
 471 has a mean absolute percentage error of 3.78%.

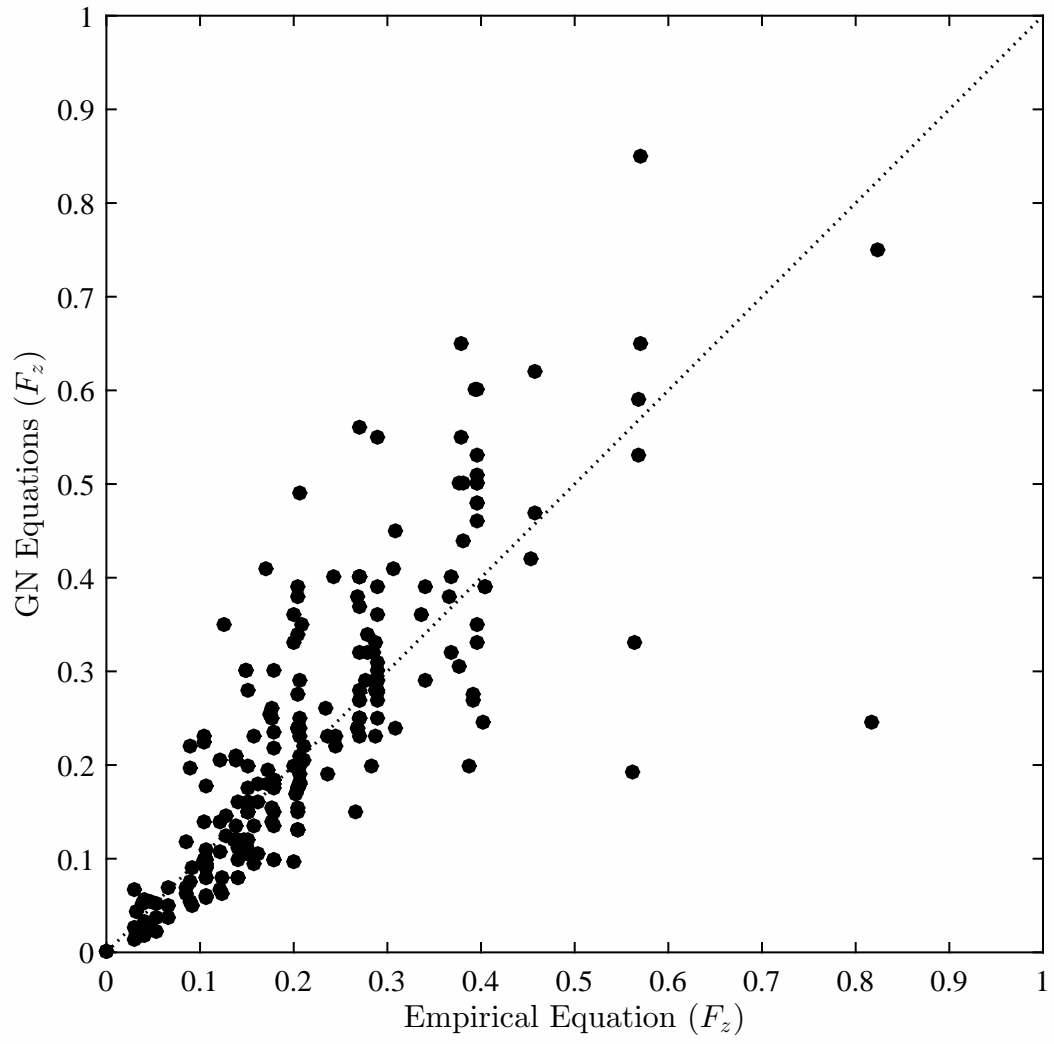


Figure 20: Agreement of the empirical equations and the GN results for the vertical uplift force.

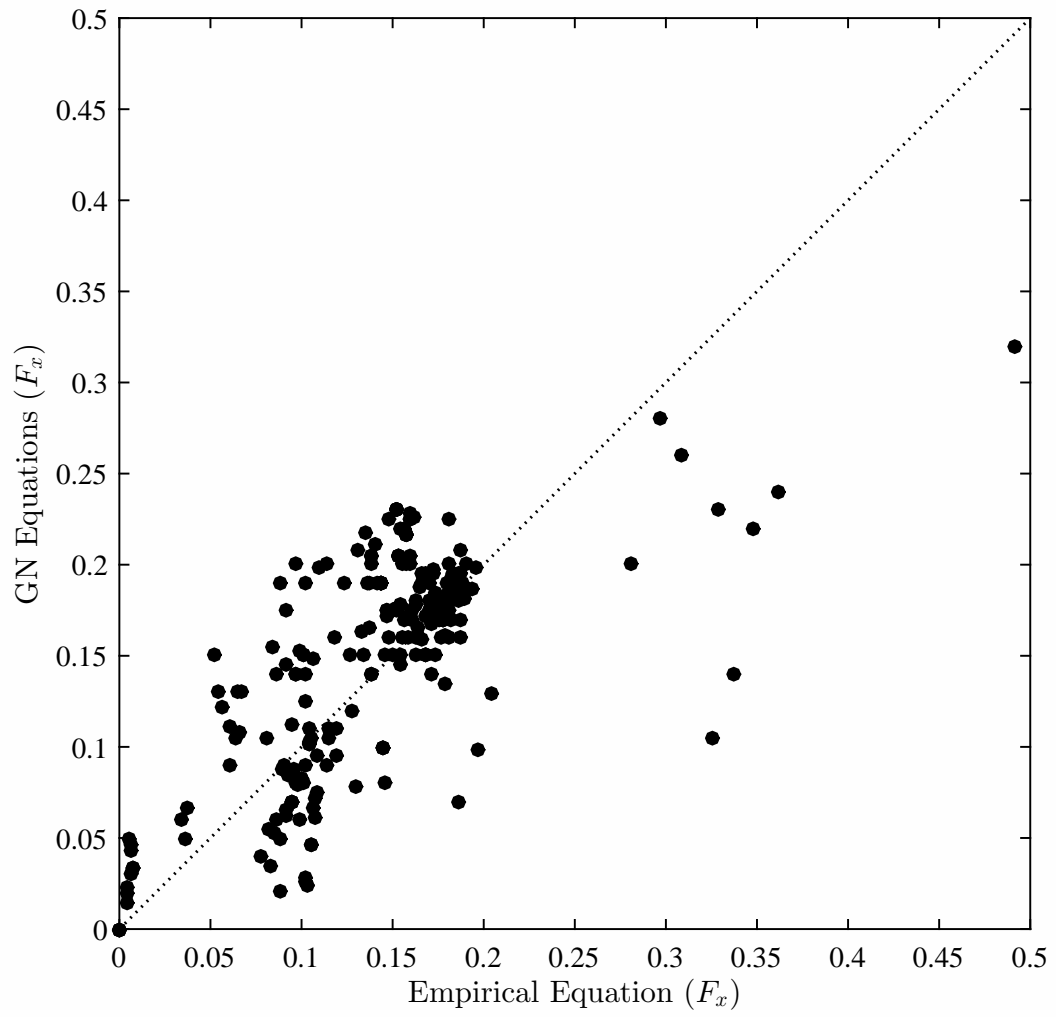


Figure 21: Agreement of the empirical equations and the GN results for the horizontal positive force.

472 We note that in this study, the wave and structure conditions are chosen
 473 such that they cover a wide range of possible and practical scenarios. How-
 474 ever, the comparisons and validations given here do not ensure applicability
 475 of the equations to cases where length scales of the wave and structure are
 476 beyond those considered.

477 7. Comparisons and Discussion

478 Comparisons of the empirical equations with the time series of forces of
 479 the GN equations, available laboratory experiments, and other theoretical
 480 and computational solutions are shown and discussed in this section.

481 Figures 22-25 show the comparison of the empirical equations with the
 482 laboratory experiments and the linear LWA solution. The laboratory exper-
 483 iments are conducted by Hayatdavoodi et al. (2015b) for a range of wave
 484 heights ($0.05 < H < 0.4$) and wave lengths ($10 < \lambda < 35$). The comparisons
 485 are given for two submergence depths ($S = 0.6$ and $S = 0.4$), and for various
 486 combinations of wave lengths, wave heights and deck lengths that may be seen
 487 in nature. Two water depths are used in the laboratory experiments, namely
 488 $h = 0.114m$ (corresponding to the results given in Figs. 22 and 23) and
 489 $h = 0.071m$ (corresponding to the results given in Figs. 24 and 25). The deck
 490 dimensions in the laboratory experiments read $L_D = 30.5\text{ cm}$, $B_D = 14.9\text{ cm}$
 491 and $t_D = 1.27\text{ cm}$. See Hayatdavoodi et al. (2015b) for further details of the
 492 laboratory experiments.

493 In all cases, results of the empirical equations are in close agreement with
 494 the laboratory measurements and the GN results. The agreement of the
 495 equation for the vertical force is better than the horizontal positive force.
 496 Overall, compared to the LWA, the empirical equations show closer agree-
 497 ment with the laboratory measurements.

498 The fluid is inviscid in the GN model, used as the basis for the devel-
 499 opment of the above empirical equations for the wave-induced vertical and
 500 horizontal forces on a submerged deck, Eqs. (5) and (6), respectively. For the
 501 cases considered here, the agreement of the GN results with the laboratory
 502 measurement show that viscosity does not play a relevant role on the forces.
 503 In this section, we provide an estimate of the magnitude of viscous forces on
 504 the submerged deck, not considered by the GN model.

505 The horizontal velocity under undisturbed, long, nonlinear cnoidal waves
 506 can be approximated by the analytical solution of velocity under a solitary
 507 wave as (see e.g. Hayatdavoodi and Ertekin (2015c)):

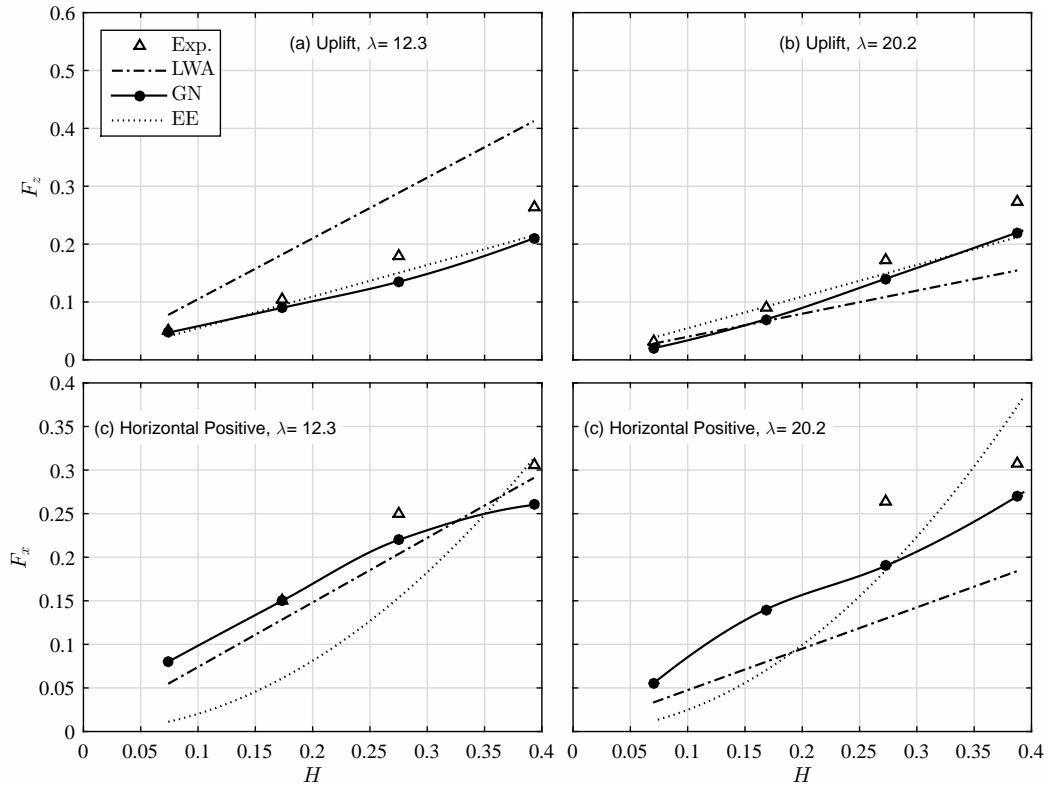


Figure 22: Comparison between laboratory measurements, GN calculations, LWA calculations and empirical equation calculations for (a) Vertical uplift and (b) horizontal positive loads on a submerged deck for cnoidal waves with different wave heights and wavelengths ($S = 0.4$; $L_D = 2.675$).

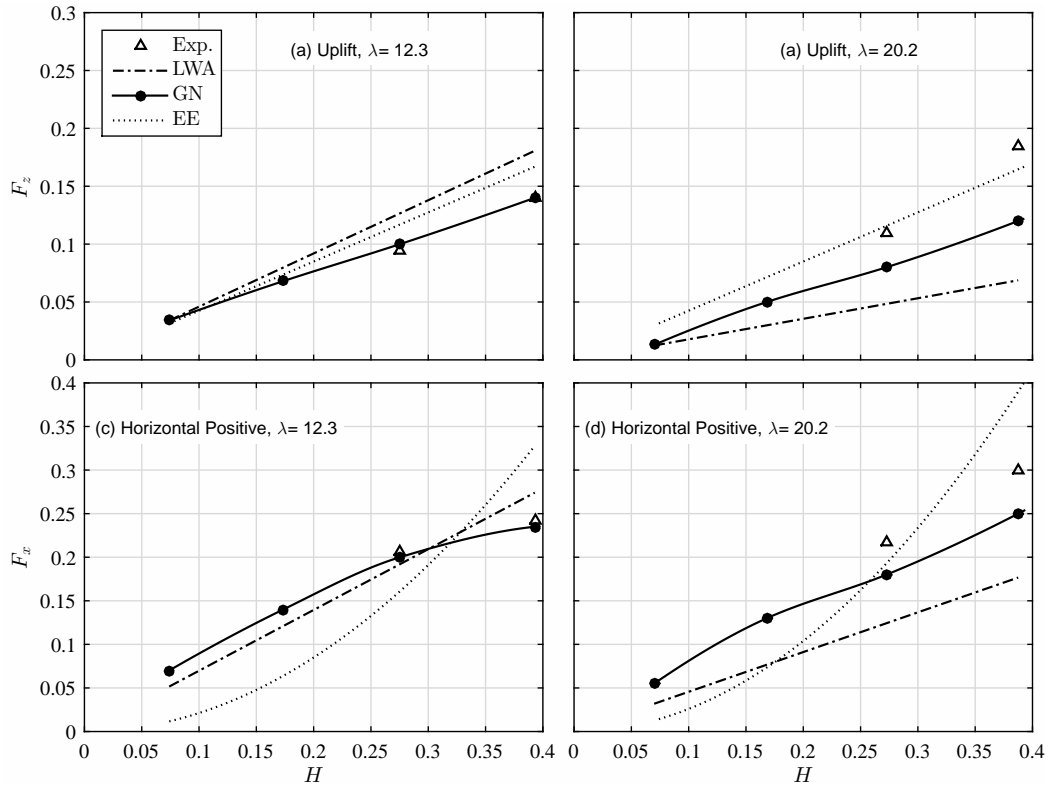


Figure 23: Comparison between laboratory measurements, GN calculations, LWA calculations and empirical equation calculations for (a) Vertical uplift and (b) horizontal positive loads on a submerged deck for cnoidal waves with different wave heights and wavelengths ($S = 0.6$; $L_D = 2.675$).

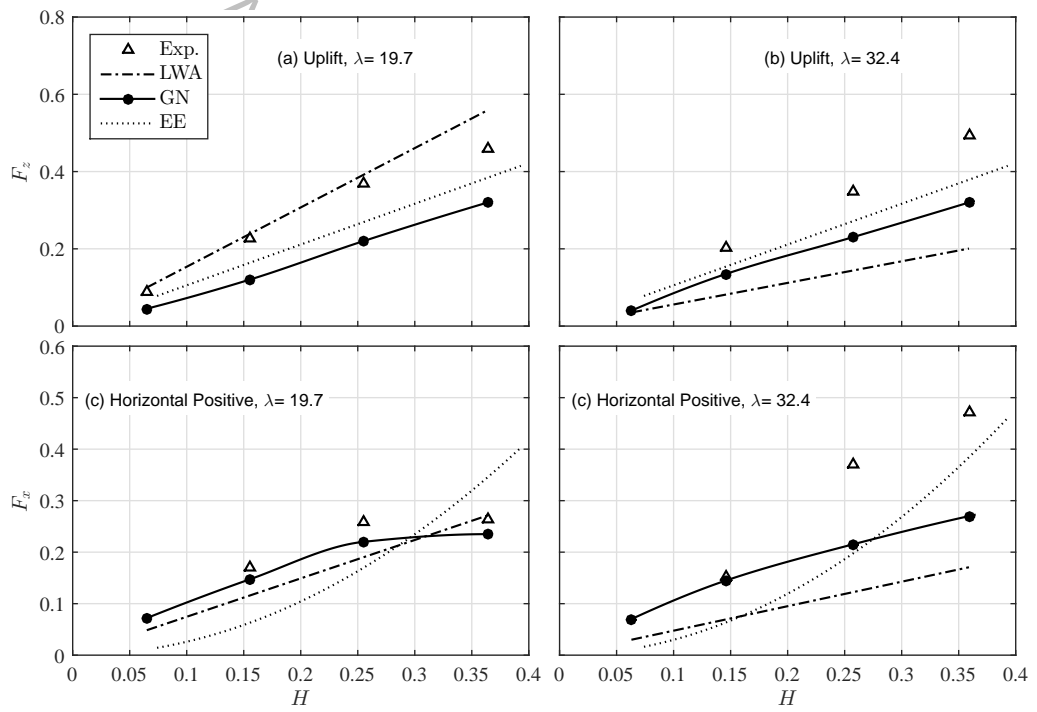


Figure 24: Comparison between laboratory measurements, GN calculations, LWA calculations and empirical equation calculations for (a) Vertical uplift and (b) horizontal positive loads on a submerged deck for cnoidal waves with different wave heights and wavelengths ($S = 0.4$; $L_D = 4.296$).

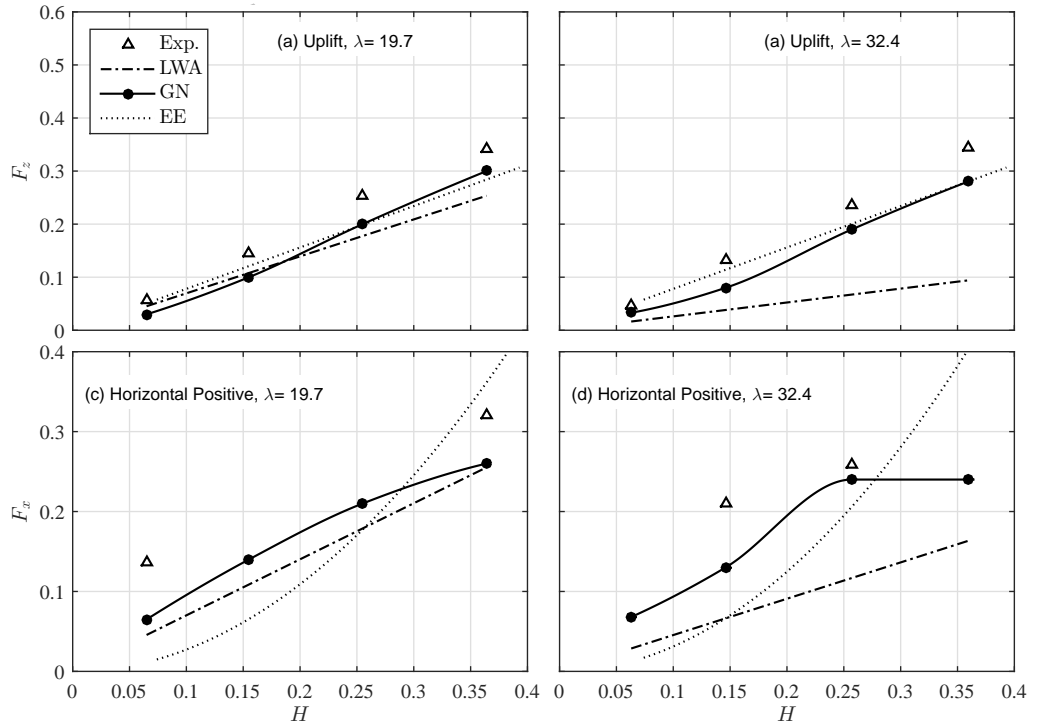


Figure 25: Comparison between laboratory measurements, GN calculations, LWA calculations and empirical equation calculations for (a) Vertical uplift and (b) horizontal positive loads on a submerged deck for cnoidal waves with different wave heights and wavelengths ($S = 0.6$; $L_D = 4.296$).

$$u(\bar{x}) = \sqrt{g(A+h)} \frac{A \operatorname{sech}^2(\epsilon \bar{x})}{h + A \operatorname{sech}^2(\epsilon \bar{x})}, \quad (7)$$

where

$$\epsilon = \sqrt{\frac{3A}{4h^2(A+h)}}, \quad (8)$$

and \bar{x} specifies the location of the crest of the wave. The maximum horizontal velocity occurs at $\bar{x} = 0$, i.e. under the wave crest. We note that the exact velocity field around the submerged deck under various wave conditions can be obtained as part of the GN solutions.

Let us consider the largest measured force on the deck in the laboratory experiments, corresponding to $H = 0.388$ and $\lambda = 20.2$ wave condition in Fig. 22, for example. Water depth in the laboratory experiments of this subfigure is $h = 0.114 \text{ m}$, see Hayatdavoodi et al. (2015b). Substituting these value into Eq. (7) gives $u = 0.35 \text{ m/s}$ for the maximum horizontal particle velocity. Hence, the maximum, local Reynolds number on the submerged plate would be approximated by $Re = uL_D/\nu = 0.35 \times 0.305/1.00 \times 10^{-6} = 1.0 \times 10^5$. Note that this is a conservative approximation of the largest force in these laboratory experiments. At this local Reynolds number, the drag force associated with the shear stresses on the submerged deck is approximated by Blasius' solution for the laminar boundary layer around a flat plate, see e.g., (Newman, 1978, Section 2.5). Hence, the skin-friction coefficient is determined by

$$C_F = \frac{1.328}{\sqrt{Re}} = 4.1 \times 10^{-3}. \quad (9)$$

Finally, the total, double-sided, frictional drag force (F_d) on the submerged plate (deck) is determined by

$$F_d = 2 \left[C_F \left(\frac{1}{2} \rho u^2 L_D \right) \right] B_D = 0.02 \text{ N}. \quad (10)$$

The dimensional magnitude of the horizontal force on the deck measured in the laboratory experiments of this case is $F_x \approx 0.66 \text{ N}$. Therefore, at the largest value, the total frictional drag force is only 3% of the measured horizontal force on the submerged deck.

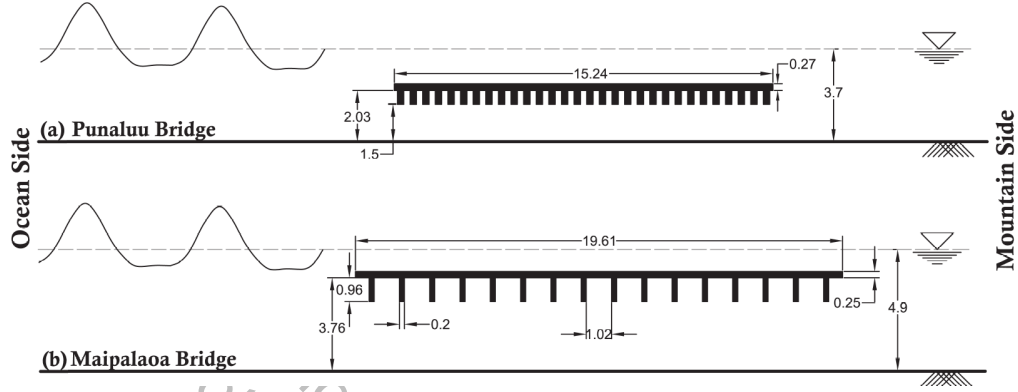


Figure 26: Two-dimensional cross sections of decks of Punaluu bridge and Maipalaoa bridge on the island of Oahu, Hawaii, USA. Dimensions are in meter. The width of one deck span (into the paper) of these bridges are (a) $B = 20.12m$ and (b) $B = 15.26m$. Girder width and spacing between girders in Punaluu bridge are 0.184 m and 0.3048 m, respectively. Also shown in this figure, are the maximum water level under extreme environmental conditions.

8. Examples: Wave Loads on Prototype Bridges

In this section, the empirical equations are used to estimate the wave loads on two prototype coastal bridges, and results are compared with the CFD and GN results of Hayatdavoodi et al. (2015a). This section is presented as a practical example on how to use the empirical equations. All variables and results are given dimensionally and in SI units.

The two coastal bridges under consideration are the Punaluu bridge and Maipalaoa bridge, both located on the island of Oahu, Hawaii, USA. Dimensions of the bridges are shown on the cross-section drawings of these bridges in Fig. 26. For these cases, the submergence depth is defined as the distance from the SWL to the middle of the bridge thickness, for which the thickness is the sum of the thickness of the deck and the height of the girders.

The extreme environmental conditions (water depth and wave conditions) at the location of these two bridges are obtained assuming large hurricanes approaching the island, and are discussed and given in Hayatdavoodi et al. (2015a). The wave conditions are given in Table 2. Note that under the extreme environmental conditions, both bridges are fully submerged.

The empirical equations (5) and (6) use dimensionless variables. Hence, the first step is to non-dimensionalize all variables as discussed in Section 3, i.e., with respect to water depth (h), water density (ρ), and gravitational

Table 2: Extreme wave conditions at the location of Punaluu bridge and Maipalaoa bridge. The submergence depth is the distance from the SWL to the middle of the deck thickness.

Bridge Name	h (m)	H (m)	T (s)	S (m)
Punaluu	3.7	2.0	6.0	1.8
Maipalaoa	4.9	2.7	6.5	1.5

acceleration (g). The dimensionless values are $\bar{H} = 0.54$, $\bar{T} = 9.77$, $\bar{S} = 0.49$ and $\bar{L}_D = 4.12$ for Punaluu bridge, and $\bar{H} = 0.55$, $\bar{T} = 9.20$, $\bar{S} = 0.31$ and $\bar{L}_D = 4.00$ for Maipalaoa bridge. Using these values in Eqs. (5) and (6) gives the dimensionless vertical uplift and horizontal positive forces of $\bar{F}_z = 0.47$ and $\bar{F}_x = 0.56$ for Punaluu bridge, and $\bar{F}_z = 0.59$ and $\bar{F}_x = 0.53$ for Maipalaoa bridge. These forces are then converted to dimensional values by use of Eq. (2), and results are compared with other solutions and shown in Figs. 27 and 28 for Punaluu and Maipalaoa bridges, respectively. Note that these are the three-dimensional forces on the bridge spans, i.e., the forces of all two-dimensional models are multiplied by the deck span width into the page.

Overall, results of the empirical equations are in good agreement with OpenFOAM results. The empirical equations have overestimated the vertical uplift force and under estimated the horizontal positive force, when compared with the CFD results. The differences, however, are within the same range as the differences between the GN and CFD results. That is, the empirical equations have provided an acceptable first estimate of the loads on the decks of the submerged bridges.

Also included in this comparison, are the results from the simplified equations of AASHTO (determined from Sections 6.1.2.2 and 6.1.2.3 of AASHTO (2008)). In the case of the Punaluu bridge, AASHTO's relations have overestimated the vertical and horizontal forces by factors larger than 10, and hence these are not shown in Fig. 27. AASHTO's relations have overestimated the vertical force on the Maipalaoa bridge by approximately a factor of 3 when compared to other results, shown in Fig. 28. These relations have underestimated the horizontal force on the Maipalaoa bridge. Other existing simplified relations, such as those suggested by Douglass et al. (2006) and McPherson (2008) are inapplicable to fully submerged decks.

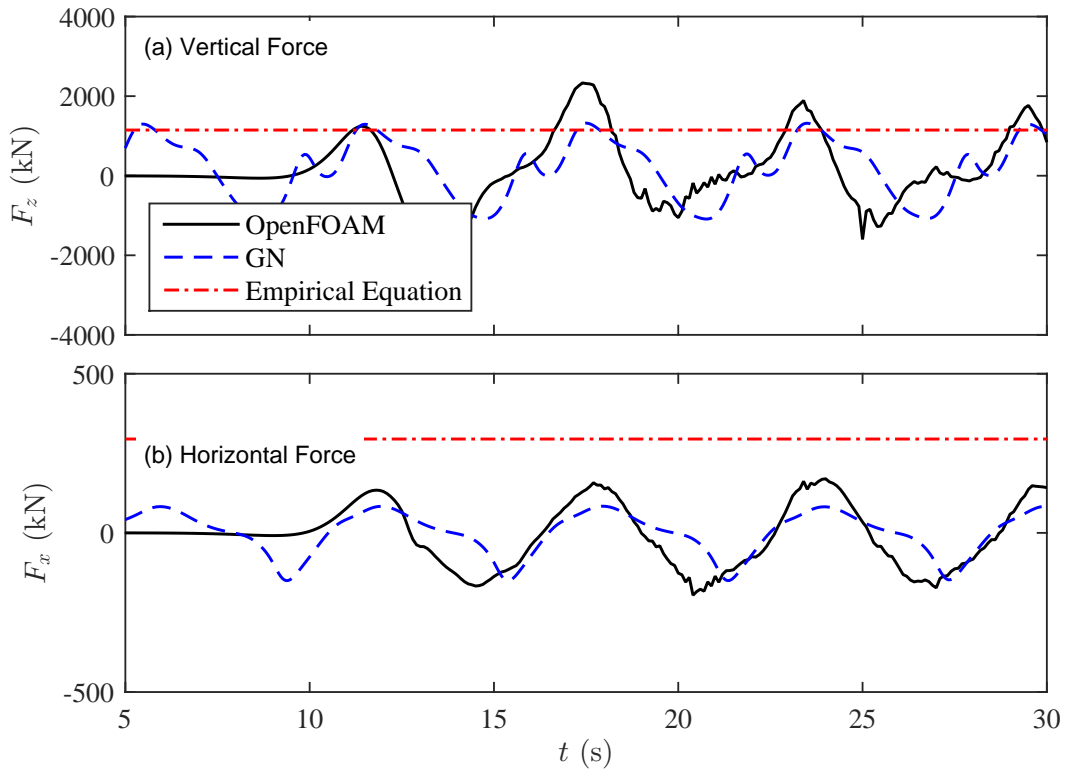


Figure 27: Comparison between OpenFOAM, GN and the empirical equations for (a) vertical force and (b) horizontal force on the Punaluu bridge.

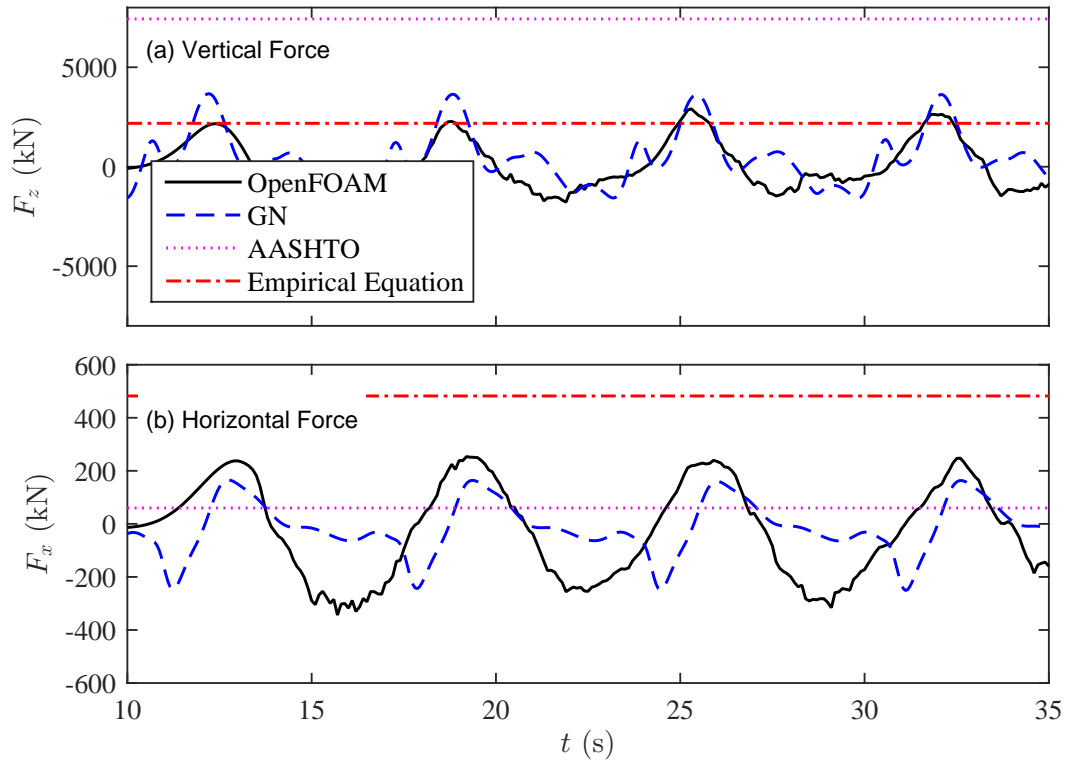


Figure 28: Comparison between OpenFOAM, GN, AASHTO and the empirical equations for (a) vertical force and (b) horizontal force on the Maipalaoa bridge.

9. Concluding Remarks

Nonlinear solitary and cnoidal wave loads on submerged, horizontal decks in shallow water are determined by use of the Level I GN equations. Results of the GN model are compared with laboratory experiments and other theoretical solutions, and a good agreement is observed.

Variation of the maximum and minimum values of the wave loads with wave height, wave period, deck submergence depth, and deck length is discussed through a parametric study. The general behaviour of the extreme values of the loads for different wave conditions and decks is an important characteristic of this problem, particularly for practical applications. The results of this parametric study, obtained for practical conditions, can be used directly to estimate the wave loads on various submerged decks in a preliminary study.

It is shown in the literature, for example by Hayatdavoodi et al. (2015a), that wave loads are the largest when the structure decks are fully submerged. To provide design engineers with simple and practical relations for estimating the wave loads, two simplified design-type empirical equations are presented based on the results of the parametric study. Overall, the empirical equations provide reasonable results when compared with laboratory experiments and CFD solutions. Note that the empirical equations provide dimensionless forces on a submerged deck. Equation (2) must be used to determine the dimensional forces, where the deck length (into the page) and deck thickness play significant role, among other variables.

The empirical equations for wave loads on submerged decks are developed based on the GN equations, considering a wide range of environmental conditions. In the absence of any scaling parameters, it is shown that results of the GN equations, and the empirical relations, compare well with the experiments and CFD results, and the models are applicable to the conditions given here. These equations are aimed to give a preliminary estimation of the loads on the decks, and do not include any safety factor. Effects of air entrapment or wave breaking, if occur, are not considered in these equations.

Acknowledgements

The work of MH and RCE is partially based on funding from State of Hawaii's Department of Transportation (HDOT) and the Federal Highway Administration (FHWA) Research Branch, Grant Nos. DOT-08-004, TA

615 2009-1R. Any findings and opinions contained in this paper are those of the
616 authors and do not necessarily reflect the opinions of the funding agencies.

Author Accepted Manuscript
Note copyedited by the Journal

References

- AASHTO, 2008. Guide Specifications for Bridges Vulnerable to Coastal Storms. American Association of State Highway and Transportation Officials, ISBN Number: 1-56051-429-9, 64 p.
- Akiyama, M., Frangopol, D.M., Arai, M., Koshimura, S., 2013. Reliability of bridges under tsunami hazards: Emphasis on the 2011 Tohoku-oki earthquake. *Earthquake Spectra* 29, S295–S314.
- Azadbakht, M., Yim, S.C., 2016. Effect of trapped air on wave forces on coastal bridge superstructures. *Journal of Ocean Engineering and Marine Energy* , 1–20.
- Boussinesq, J., 1871. Theorie de l'intumescence liquide appele onde solitaire ou de translation. *Comptes Rendus Acad. Sci. Paris* 72, 755–759.
- Bradner, C., Schumacher, T., Cox, D., Higgins, C., 2011. Experimental setup for a large-scale bridge superstructure model subjected to waves. *J. of Waterway, Port, Coastal, and Ocean Engineering* 137, 3–11.
- Brater, E.F., McNown, J.S., Stair, L.D., 1958. Wave forces on submerged structures. *J. of the Hydraulics Division, ASCE* 84, 1–26.
- Bricker, J.D., Nakayama, A., 2014. Contribution of trapped air, deck super-elevation, and nearby structures to bridge deck failure during a tsunami. *J. of Hydraulic Engineering* 140, 05014002 (1–7).
- Carter, R.W., Ertekin, R.C., 2014. Focusing of wave-induced flow through a submerged disk with a tubular opening. *Applied Ocean Research* 47, 110–124.
- Chu, C.R., Chung, C.H., Wu, T.R., Wang, C.Y., 2016. Numerical analysis of free surface flow over a submerged rectangular bridge deck. *Journal of Hydraulic Engineering* 142, 04016060.
- Douglass, S.L., Chen, Q., Olsen, J.M., Edge, B.L., Brown, D., 2006. Wave forces on bridge decks. Univ. of South Alabama, Coastal Transportation Engineering Research and Education Center, Univ. of South Alabama, Mobile, Ala, vi+74 p.

- 647 Durgin, W.W., Shiau, J.C., 1975. Wave induced pressures on submerged
648 plates. *J. of Waterways, Harbor, and Coastal Engineering*, ASCE 101,
649 59–71.
- 650 Ertekin, R.C., 1984. Soliton Generation by Moving Disturbances in Shallow
651 Water: Theory, Computation and Experiment. Ph.D. thesis. University of
652 California at Berkeley, May, v+352 p. University of California at Berkeley.
- 653 Ertekin, R.C., Riggs, H.R., Che, X.L., Du, S.X., 1993. Efficient methods for
654 hydroelastic analysis of very large floating structures. *J. Ship Research* 37,
655 58–76.
- 656 Ertekin, R.C., Webster, W.C., Wehausen, J.V., 1986. Waves caused by
657 a moving disturbance in a shallow channel of finite width. *J. of Fluid*
658 *Mechanics* 169, 275–292.
- 659 Graw, K., 1993. Shore protection and electricity by submerged plate wave en-
660 ergy converter, in: *Proceedings of the European wave energy symposium*.
661 Edinburgh, Scotland, pp. 379–384.
- 662 Green, A.E., Naghdi, P.M., 1974. On the theory of water waves. *Proceed-*
663 *ings of the Royal Society of London. Series A, Mathematical and Physical*
664 *Sciences* 338, 43–55.
- 665 Green, A.E., Naghdi, P.M., 1976. Directed fluid sheets. *Proceedings of the*
666 *Royal Society of London. Series A, Mathematical and Physical Sciences*
667 347, 447–473.
- 668 Green, A.E., Naghdi, P.M., 1984. A direct theory of viscous fluid flow in
669 channels. *Archive for Rational Mechanics and Analysis* 86, 39–63.
- 670 Guo, A., Fang, Q., Bai, X., Li, H., 2015a. Hydrodynamic experiment of the
671 wave force acting on the superstructures of coastal bridges. *Journal of*
672 *Bridge Engineering* 20, 04015012 (1–11).
- 673 Guo, A., Fang, Q., Li, H., 2015b. Analytical solution of hurricane wave forces
674 acting on submerged bridge decks. *Ocean Engineering* 108, 519–528.
- 675 Hayatdavoodi, M., 2013. Nonlinear wave loads on decks of coastal structures.
676 Ph.D. thesis. University of Hawaii at Manoa, xiv+186 p. University of
677 Hawaii at Manoa.

- 678 Hayatdavoodi, M., Ertekin, R.C., 2015a. Nonlinear wave loads on a sub-
679 merged deck by the Green-Naghdi equations. *J. of Offshore Mechanics*
680 *and Arctic Engineering* 137, 011102 (1–9), DOI: 10.1115/1.4028997.
- 681 Hayatdavoodi, M., Ertekin, R.C., 2015b. Wave forces on a submerged hor-
682 izontal plate. Part I: Theory and modelling. *J. of Fluids and Structures*
683 54, 566–579, DOI: 10.1016/j.jfluidstructs.2014.12.010.
- 684 Hayatdavoodi, M., Ertekin, R.C., 2015c. Wave forces on a submerged hori-
685 zontal plate. Part II: Solitary and cnoidal waves. *J. of Fluids and Structures*
686 54, 580–596, DOI: 10.1016/j.jfluidstructs.2014.12.009.
- 687 Hayatdavoodi, M., Ertekin, R.C., 2016. Review of wave loads on coastal
688 bridge decks. *Applied Mechanics Reviews* 68, 030802 (1–16). DOI:
689 10.1115/1.4033705.
- 690 Hayatdavoodi, M., Ertekin, R.C., Robertson, I.N., Riggs, H.R., 2015a. Vul-
691 nerability assessment of coastal bridges on Oahu impacted by storm surge
692 and waves. *Natural Hazards* , 1–25, DOI: 10.1007/s11069-015-1896-2.
- 693 Hayatdavoodi, M., Ertekin, R.C., Thies, J.T., 2017a. Conceptual design and
694 analysis of a submerged wave energy device in shallow water, in: 36th
695 Int. Conf. on Ocean, Offshore and Arctic Engineering, OMAE '17, ASME,
696 June 25-30, Trondheim, Norway, OMAE2017-62174.
- 697 Hayatdavoodi, M., Ertekin, R.C., Valentine, B.D., 2017b. Solitary and
698 cnoidal wave scattering by a submerged horizontal plate in shallow wa-
699 ter. *AIP Advances* 7, 065212.
- 700 Hayatdavoodi, M., Neill, D.R., Ertekin, R.C., 2018. Diffraction of cnoidal
701 waves by vertical cylinders in shallow water. *Theoretical and Computa-*
702 *tional Fluid Dynamics* 32, 561–591.
- 703 Hayatdavoodi, M., Seiffert, B., Ertekin, R.C., 2014. Experiments
704 and computations of Solitary-Wave forces on a coastal-bridge deck.
705 Part II: Deck with girders. *Coastal Engineering* 88, 210–228, DOI:
706 10.1016/j.coastaleng.2014.02.007.
- 707 Hayatdavoodi, M., Seiffert, B., Ertekin, R.C., 2015b. Experiments and cal-
708 culations of cnoidal wave loads on a flat plate in shallow-water. *J. of Ocean*

709 Engineering and Marine Energy 1, 77–99, DOI: 10.1007/s40722-014-0007-
710 X.

711 He, H., Troesch, A.W., Perlin, M., 2008. Hydrodynamics of damping plates at
712 small kc numbers, in: IUTAM Symposium on Fluid-Structure Interaction
713 in Ocean Engineering, Hamburg, Germany, Springer. pp. 93–104.

714 Herbich, J.B., Shank, G.E., 1970. Forces due to waves on submerged struc-
715 tures theory and experiment, in: Offshore Technology Conference, Hous-
716 ton, Texas, pp. 189–202.

717 HYDRAN, 2012. A computer program for the hydroelastic response analysis
718 of ocean structures. Technical Report. Offcoast Inc., Kailua, HI, September
719 2012. ver. 5.1.7.

720 Iemura, H., Pradono, M.H., Takahashi, Y., 2005. Report on the tsunami
721 damage of bridges in Banda Aceh and some possible countermeasures.
722 Proceedings of the 27th Earthquake Engineering Symposium 28, 214–214.

723 Kerenyi, K., Sofu, T., Guo, J., 2009. Hydrodynamic Forces on Inundated
724 Bridge Decks. Technical Report EHWA-HRT-09-028. Turner-Fairbank
725 Highway Research Center, 38 p.

726 Kojima, H., Yoshida, A., Nakamura, T., 1994. Linear and nonlinear wave
727 forces exerted on a submerged horizontal plate. Proceedings of 24th Con-
728 ference on Coastal Engineering, Kobe, Japan , 1312–1326.

729 Kosa, K., 2011. Damage analysis of bridges affected by tsunami due to
730 Great East Japan earthquake, in: Proceedings of the 27Th U.S.-Japan
731 Bridge Engineering Workshop, pp. 55–65.

732 Kulin, G., 1958. Solitary Wave Forces on Submerged Cylinders and Plates.
733 Technical Report. National Bureau of Standards, Volume 5876, 44 p.

734 Liu, P.L.F., Iskandarani, M., 1991. Scattering of short-wave groups by sub-
735 merged horizontal plate. J. of Waterway, Port, Coastal, and Ocean Engi-
736 neering 117, 235–246.

737 Lo, H.Y., Liu, P.L., 2014. Solitary waves incident on a submerged horizontal
738 plate. J. of Waterway Port Coastal and Ocean Engineering 140, 04014009
739 (1–17).

- 740 McIver, M., 1985. Diffraction of water waves by a moored, horizontal, flat
741 plate. *J. of Engineering Mathematics* 19, 297–319.
- 742 McPherson, R.L., 2008. Hurricane Induced Wave and Surge Forces on Bridge
743 Decks. Master’s thesis. Texas A&M University, xii+90 p.
- 744 Morison, J.R., O’Brien, M.P., Johnson, J.W., Schaaf, S.A., 1950. The force
745 exerted by surface piles. *Petroleum Transactions* Vol. 189, 149–154.
- 746 Needham, H., 2017. Hurricane Harvey. www.u-surge.net.
- 747 Neill, D.R., Hayatdavoodi, M., Ertekin, R.C., 2018. On solitary wave diffrac-
748 tion by multiple, in-line vertical cylinders. *Nonlinear Dynamics* 91, 975–
749 994.
- 750 Newman, J.N., 1978. *Marine Hydrodynamics*. Cambridge: MIT Press. 2nd
751 edition.
- 752 Park, H., Tomiczek, T., Cox, D.T., van de Lindt, J.W., Lomonaco, P., 2017.
753 Experimental modeling of horizontal and vertical wave forces on an ele-
754 vated coastal structure. *Coastal Engineering* 128, 58 – 74.
- 755 Patarapanich, M., 1984. Forces and moment on a horizontal plate due to
756 wave scattering. *Coastal Engineering* 8, 279 – 301.
- 757 Rey, V., Touboul, J., 2011. Forces and moment on a horizontal plate due
758 to regular and irregular waves in the presence of current. *Applied Ocean*
759 *Research* 33, 88 – 99.
- 760 Riggs, H.R., Suzuki, H., Ertekin, R.C., Kim, J.W., Iijima, K., 2008. Compar-
761 ison of hydroelastic computer codes based on the ISSC VLFS benchmark.
762 *Ocean Engineering* 35, 589 – 597.
- 763 Robertson, I.N., Riggs, H.R., Yim, S.C., Young, Y.L., 2007. Lessons from
764 Hurricane Katrina storm surge on bridges and buildings. *J. of Waterway,*
765 *Port, Coastal, and Ocean Engineering* 133, 463–483.
- 766 Schember, H.R., 1982. A new model for three-dimensional nonlinear disper-
767 sive long waves. Ph.D. thesis. California Institute of Technology, Pasadena.

- 768 Schumacher, T., Higgins, C., Bradner, C., Cox, D., Yim, S.C., 2008. Large-
769 scale wave flume experiments on highway bridge superstructures exposed
770 to hurricane wave forces, in: The Sixth National Seismic Conference on
771 Bridges & Highways, Charleston, South Carolina, Charleston, South Car-
772 olina.
- 773 Seiffert, B., Hayatdavoodi, M., Ertekin, R.C., 2014. Experiments and compu-
774 tations of solitary-wave forces on a coastal-bridge deck. Part I: Flat plate.
775 Coastal Engineering 88, 194–209, DOI: 10.1016/j.coastaleng.2014.01.005.
- 776 Siew, P.F., Hurley, D.G., 1977. Long surface waves incident on a submerged
777 horizontal plate. J. of Fluid Mechanics 83, 141–151.
- 778 Tao, L., Dray, D., 2008. Hydrodynamic performance of solid and porous
779 heave plates. Ocean Engineering 35, 1006–1014.
- 780 Unjoh, S., 2006. Damage investigation of bridges affected by tsunami dur-
781 ing 2004 north Sumatra earthquake, Indonesia, in: Fourth International
782 Workshop on Seismic Design and Retrofit of Transportation Facilities, San
783 Francisco, California.
- 784 Webster, W.C., Wehausen, J.V., 1995. Bragg scattering of water waves by
785 Green-Naghdi theory, in: Casey, J., Crochet, M. (Eds.), Theoretical, Ex-
786 perimental, and Numerical Contributions to the Mechanics of Fluids and
787 Solids. Birkhuser Basel, pp. 566–583.
- 788 Webster, W.C., Zhao, B., 2018. The development of a high-accuracy, broad-
789 band, Green–Naghdi model for steep, deep-water ocean waves. Journal of
790 Ocean Engineering and Marine Energy 4, 273–291.
- 791 Whitham, G.B., 1974. Linear and Nonlinear Waves. Prentice-Hall Inc. /
792 Englewood Cliffs, N.J., xi + 532 pp.
- 793 Wu, D., Wu, T.Y., 1982. Three-dimensional nonlinear long waves due to
794 moving surface pressure, in: Proc. 14th Symp. on Naval Hydrodynamics,
795 Washington, D.C., National Academy Press, Washington, D.C., 1983. pp.
796 103–125.
- 797 Xu, G., Cai, C.S., Han, Y., 2015. Investigating the characteristics of the
798 solitary wave-induced forces on coastal twin bridge decks. Journal of Per-
799 formance of Constructed Facilities , 04015076(1–17).

800 Zitti, G., Ancey, C., Postacchini, M., Brocchini, M., 2016. Impulse waves
801 generated by snow avalanches: Momentum and energy transfer to a water
802 body. *Journal of Geophysical Research: Earth Surface* 121, 2399–2423.

Author Accepted Manuscript
Note copyedited by the Journal